patients with myocardial ischemia (Lambiase *et al*, 2004). In this study, we show, for the first time, a correlation between neovascularization of the cerebral arterial circulation and increased levels of circulating CD34+ cells. Our results support the hypothesis that circulating CD34+ cells potentially contribute to neovascularization at sites of ischemic brain injury.

Acknowledgements

We thank K Obata and Y Okinaka for technical assistance.

Conflict of interest

The authors state no conflict of interest.

References

Borlongan CV, Lind JG, Dillon-Carter O, Yu G, Hadman M, Cheng C, Carroll J, Hess DC (2004*a*) Bone marrow grafts restore cerebral blood flow and blood brain barrier in stroke rats. *Brain Res* 1010:108–16

Borlongan CV, Lind JG, Dillon-Carter O, Yu G, Hadman M, Cheng C, Carroll J, Hess DC (2004*b*) Intracerebral xenografts of mouse bone marrow cells in adult rats facilitate restoration of cerebral blood flow and blood–brain barrier. *Brain Res* 1009:26–33

Boyle AJ, Whitbourn R, Schlicht S, Krum H, Kocher A, Nandurkar H, Bergmann S, Daniell M, O'Day J, Skerrett D, Haylock D, Gilbert RE, Itescu S (2006) Intra-coronary high-dose CD34+ stem cells in patients with chronic ischemic heart disease: a 12-month follow-up. *Int J Cardiol* 109:21–7

Kudo FA, Nishibe T, Nishibe M, Yasuda K (2003) Autologous transplantation of peripheral blood endothelial progenitor cells (CD34+) for therapeutic angiogenesis in patients with critical limb ischemia. *Int Angiol* 22:344–8

Lambiase PD, Edwards RJ, Anthopoulos P, Rahman S, Meng YG, Bucknall CA, Redwood SR, Pearson JD, Marber MS (2004) Circulating humoral factors and endothelial progenitor cells in patients with differing coronary collateral support. *Circulation* 109:2986–92

Majka M, Janowska-Wieczorek A, Ratajczak J, Ehrenman K, Pietrzkowski Z, Kowalska MA, Gewirtz AM, Emerson SG, Ratajczak MZ (2001) Numerous growth factors, cytokines, and chemokines are secreted by human CD34(+) cells, myeloblasts, erythroblasts, and megakaryoblasts and regulate normal hematopoiesis in an autocrine/paracrine manner. *Blood* 97:3075–85

Natori Y, Ikezaki K, Matsushima T, Fukui M (1997) 'Angiographic moyamoya' its definition, classification, and therapy. *Clin Neurol Neurosurg* 99(Suppl 2): S168–72

Taguchi A, Matsuyama T, Moriwaki H, Hayashi T, Hayashida K, Nagatsuka K, Todo K, Mori K, Stern DM, Soma T, Naritomi H (2004*a*) Circulating CD34-positive cells provide an index of cerebrovascular function. *Circulation* 109:2972–5

Taguchi A, Matsuyama T, Nakagomi T, Shimizu Y, Fukunaga R, Tatsumi Y, Yoshikawa H, Kikuchi-Taura A, Soma T, Moriwaki H, Nagatsuka K, Stern DM, Naritomi H (2007) Circulating CD34-positive cells provide a marker of vascular risk associated with cognitive impairment. *J Cereb Blood Flow Metab*; e-pub ahead of print 8 August 2007

Taguchi A, Ohtani M, Soma T, Watanabe M, Kinosita N (2003) Therapeutic angiogenesis by autologous bone-marrow transplantation in a general hospital setting. *Eur J Vasc Endovasc Surg* 25:276–8

Taguchi A, Soma T, Tanaka H, Kanda T, Nishimura H, Yoshikawa H, Tsukamoto Y, Iso H, Fujimori Y, Stern DM, Naritomi H, Matsuyama T (2004*b*) Administration of CD34+ cells after stroke enhances neurogenesis via angiogenesis in a mouse model. *J Clin Invest* 114:330–8

Available online at www.sciencedirect.com
ScienceDirect
Behavioural Brain Research 179 (2007) 90–98
BEHAVIOURAL BRAIN RESEARCH
www.elsevier.com/locate/bbr

Research report

Environmental change during postnatal development alters behaviour, cognitions and neurogenesis of mice

Hiroyuki Iso [a,*], Shigero Simoda [a], Tomohiro Matsuyama [b]

[a] *Department of Behaviour Science, Hyogo College of Medicine, 1-1 Mukogawa-cho, Nishinomiya, Hyogo 663-8501, Japan*
[b] *Institute for Advanced Medical Sciences, Hyogo College of Medicine, 1-1 Mukogawa-cho, Nishinomiya, Hyogo 663-8501, Japan*

Received 22 March 2006; received in revised form 4 January 2007; accepted 23 January 2007
Available online 3 February 2007

Abstract

Four groups of male C57BL/6 mice were reared differing combinations of the two environments from 3 to 11 weeks after birth. At 12 and 13 weeks they were assessed by measures of behaviour and learning: open-field activity, auditory startle reflex and prepulse inhibition, water maze learning, and passive avoidance. Another four groups of mice reared under these varying conditions were examined for generation of neurons in hippocampus and cerebral cortex using bromodeoxyuridine (BrdU) at 12 weeks. Enriched (EE) and impoverished (PP) groups were housed in their respective environment for 8 weeks, enriched–impoverished (EP) and impoverished–enriched (PE) mice respectively were reared for 6 weeks in the first-mentioned environment and then for 2 weeks in the second. PP and EP mice showed hyperactivity, greater startle amplitude and significantly slower learning in a water maze than EE or PE animals, and also showed a memory deficit in a probe test, avoidance performance did not differ. Neural generation was greater in the EE and PE than PP and EP groups, especially in the hippocampus. These results suggest that environmental change critically affects behavioural and anatomic brain development, even if brief. In these mice, the effect of unfavourable early experience could be reversed by a later short of favourable experience.

Keywords: Enrichment; Impoverishment; Environmental change; Behaviour; Neuronal generation; Mice

1. Introduction

Research concerning environmental enrichment has been carried out since 1960s. Earlier studies reported that rats reared for a few months following weaning in a group in a large cage with a running wheel, toys and a hiding had greater brain weights and showed more acetylcholinesterase activity than animals reared alone in a small cage for the same period even though both environments had food and water continuously available [38,40]. Some authors suspected that an increase in glial cells might have contributed to these differences [2]. Later, rats spending earlier life in an enriched environment had been reported to show lower activity in open field test than rats spending the same period in an impoverished setting with little stimulation [17]. Still other reports indicated that even brief exposure to the enriched environment affected development of brain and behaviour in rats [11,12]. In recent studies involving rats, an enriched developmental environment was reported to increase neurotrophic factor gene expression [29], brain-derived neurotrophic factor protein [30], numbers of hippocampal neurons [20,21,48,49], and dendritic growth, in association with improvements in behaviour and cognition [22]. Recovery from transient global ischemia was reported clinically to be promoted by environment enrichment [15]. Environmental enrichment also was reported to promote normal emotional behaviour and even immune function under stress [5]. Even "knockout" mice with a genetically mediated hippocampal deficit causing behavioural and memory deficiencies were reported to improve their ability to learn after a period of exposure to an enriched environment [8,35]. Thus, a benefit from environmental enrichment during development of animals concerning behaviour, neurophysiology, neuroanatomy, and even immunity has been reported and even applied to humans [16,36,37].

On the other hand, some authors point out that an enriched environment is the natural situation in animal neurologic development, while environmental impoverishment is an artificial

Abbreviations: BrdU, 5-bromo-2′-deoxyuridine; PSA-NCAM, polysialylated neuronal cell adhesion molecule

* Corresponding author. Tel.: +81 798456378; fax: +81 798456378.
E-mail address: iso@hyo-med.ac.jp (H. Iso).

0166-4328/$ – see front matter © 2007 Elsevier B.V. All rights reserved.
doi:10.1016/j.bbr.2007.01.025

condition inducing neurologic maldevelopment [27,41]. Indeed, rats housed singly can show abnormal behaviours, such as attention deficiency, hyperactivity, exaggerated emotional behaviour, and stereotypy [6,51], accompanied by evidence of neurochemical change [24,31,32]. Lack of manipulation during infancy also was reported to impair learning and memory in the adult rat [34]. Socially isolated animals even have been studied as a model of human psychotic illness [6]. Some animal studies also have examined whether or not resocialization could reverse effects of social isolation. Hyperactivity and hypoanalgesia [14] as well as deficient in water-maze learning [50] in impoverished rats has been demonstrated to be reversible upon resocialization. However, other studies where impoverishment started at weaning period failed to show this effect [9,13], suggest that the developing brain is susceptible to permanent changes at an earlier age. Wright et al. [51] reported that rats reared in an impoverished environment for 30 days after weaning, could not reverse their profile of anxious behaviour in X-maze performance after resocialization for 30 days. The performance of rats experiencing the reverse condition (a change from enriched to impoverished environments) did not differ from that in the enrichment group. Thus, reversal of environmental conditions 30 days after weaning did not affect the animals' emotional profiles. Katz and Davies [19] tested the effects of environmental manipulation during developing period on the neuroanatomy of the rats using a factorial design. Two groups of animals were reared in the enriched or impoverished environment for 2 months. Another two groups of rats were housed enriched or impoverished environment for 1 month, then the housing condition was changed to impoverished or enriched in the next month, respectively. The neuroanatomical outcomes of the enriched and impoverished groups supported to earlier reports by Rosenzweig et al. [38,40] that enriched rats had heavier brain weight, longer cerebral length and greater cortical thickness than impoverished rats. The results of the two exchange groups showed that animals which experienced enriched housing whichever during early or later 1 month developed their brain as same as the enriched group. Thus, enrichment was beneficial for brain development, and development of the brain was not modified by impoverishment, once rats had experienced enrichment [19].

The finding of neurogenesis in the adult rat [43,44] involves methods for discriminating newly generated neurons from established cell masses in the various areas of the brain. Much evidence has accumulated about effects of environment on brain development [2,21–23,29,30,38]. Additionally, experience with running was reported to enhance neurogenesis and promoted long-term potentiation (LTP) and learning in mice [47,48]. Yet, little has been known about effects of environmental manipulation during development on generation of neurons in adult rodents [20,21,48,49].

Whether enrichment or impoverishment is a more important environmental influence on neural development, neuronal plasticity suggests that exposure of impoverished animals to an enriched environment will enhance behavioural performance, while the reverse sequence will impair performance even if it is a short duration [11,12]. The objects of the present experiment are to test whether the environmental manipulations, from enrichment to impoverishment, or impoverishment to enrichment affect to the behavioural and neuronal development in mice [19], because we have experienced behavioural and neuroanatomical experiments in mice [25,52,53,1,45] and mice were drawn attention as models of human behavioural and psychiatric diseases rather than rats due to the developing evidences by gene engineering [7].

2. Materials and methods

All procedures were performed in accordance with National Cardiovascular Center Animal Care and Use Protocol. Quantitative measurements including behavioural tests and microscopic assessments were performed by investigators without knowing identity of the animal or section under study.

2.1. Experiment 1: behaviour

The effect of environmental manipulations on activity, reflexes, attention and cognition, spatial learning and of memory of fear were examined.

2.1.1. Subjects

Forty-four male C57BL/6 mice, purchased from Nihon SLC (Shizuoka Japan) of age at 3 weeks were reared under four different housing conditions for 8 weeks. Tap water and food (MF chow, Oriental, Tokyo Japan) were continuously available. In the enriched (EE) group, mice were housed for 8 weeks four animals to a plastic cage (60 cm × 80 cm × 30 cm) containing plastic tubes as toys, a hiding place, and a running wheel. Mice in the impoverished (PP) group were housed for 8 weeks singly in a small plastic cage (20 cm × 30 cm × 20 cm) with no play materials. Enriched–impoverished (EP) mice first were housed like EE mice for 6 weeks and then like PP mice for 2 weeks. Impoverished–enriched (PE) mice were housed like PP mice for 6 weeks and then like EE mice for 2 weeks. Mice were handled once weekly for less than 1 min to weigh them and place them in clean cages. The two connected rooms where mice were housed and tested were air conditioned to maintain temperatures between 20 and 21 °C. Room lights were on from 7 a.m. to 7 p.m.

2.2. Apparatus and experimental protocol

Behavioural tests (one to four below) were conducted in order of description (and of increasing complexity) to avoid order effects [26]. The basic experimental settings of the open-field test, Morris water maze learning and passive avoidance task were reported previously [25,52]. All the behavioural tests were conducted during light period (10:00–16:00 h), and the group order of animals applied to each test was random. Mixed-type analyses of variance (ANOVA) were used for data analysis. Differences between groups were tested further with a post hoc test (Bonferroni/Dunn, with $p < .05$ defining significance).

2.2.1. Open-field test

Animals were allowed to move freely in a square acrylic box (30 cm × 30 cm) for 20 min. Ten minutes light period was followed by 10-min dark period. On X and Y sides of the open-field, two infrared beams were positioned 2 cm above the box floor at a 10-cm distance. A flip-flop circuit was set up between the two beams. The total number of beam crossings was counted as locomotive behaviour of the animal. On the X side, 12 other infrared beams were positioned 5 cm above the floor at 3-cm intervals, and the total number of beam crossings was counted as rearing behaviour. After the session, stools left on the floor were counted.

2.2.2. Acoustic startle reflex and prepulse inhibition test

Basic experimental settings were reported previously [42,53], we modified these for the present study. Briefly, the mouse was placed in a translucent acrylic cage (7 cm × 7 cm × 16.5 cm). Movements of the animal were detected by a piezoelectric accelerometer (GH313A, GA245SO; Keyence, Kyoto, Japan) attached at the bottom of cage. White noise at 115 dB (c) with duration of 50 ms was used as the acoustic startle stimulus (pulse). A noise prepulse of 85 dB (c)

was presented for 30 ms. Background noise was kept at a relatively constant level, 70–73 dB (c). The test session consisted of a total of 64 trials: 40 startle trials (habituation) without a prepulse, followed by 24 trials of prepulse test session. The mean inter-trial interval was 25 s (range, 15–45 s). In the prepulse trials prepulse with lead times of 50, 100, or 200 ms was followed by the pulse. In the prepulse test session, 12 pulse-alone trials and 12 prepulse trials were presented in random order. Relative startle response (RSR) was calculated using the formula RSR = PP/*N*, where PP designated the mean response with a prepulse, and *N* designated the mean response without a prepulse.

2.2.3. Water maze learning

A swimming tank 96 cm in diameter was used. Nontoxic India ink was added to the water to render it opaque. Water temperature was maintained at 20–24 °C. A platform 10 cm in diameter was positioned at a consistent point in the tank, submerged 5 mm below the surface of the water. In the learning trial, a mouse was placed in one of the three quadrants of the pool without platform. The experimenter determined the swimming time until reaching the platform (latency) using a stopwatch. When the animal reached the platform it was allowed to stay there for 10 s, and then was returned to a waiting box. If a mouse could not reach the platform within 60 s, the mouse was placed on the platform by the experimenter, and the latency was taken to be 60 s. The interval between trials was 30 s.

2.2.4. Passive avoidance learning

The apparatus consisted of two compartments, one lit and one dark, separated by a vertically sliding door. Mice initially were placed in the lit compartment. After the door was opened and the animal entered the dark compartment, the door was closed. After 10 s, a 3-s, 0.6-mA shock was delivered. The mouse was allowed to recover for 10 s and then returned to the home cage. Twenty-four hours later the mouse again was placed in the lit section with the door positioned opened to allow movement into the dark section. Latencies for stepping through the door were recorded.

2.2.5. Assessment of brain weight

After all behavioural tests, mice were killed by cervical dislocation. The brain was removed including the olfactory bulbs, the brainstem was cut at the level of the foramen magnum. Brain weighted at exactly 3 min after cervical dislocation.

2.3. Experiment 2: neuroanatomy

The effect of environmental manipulations on generation of neurons was examined using new mice.

2.3.1. Subjects

Twenty-eight male C57BL/6 mice, purchased from Nihon SLC (Shizuoka, Japan) when 3 weeks old, were reared for 8 weeks in four groups (each $n = 7$) with different housing conditions in the same manner as Experiment 1. Tap water and food (MF chow, Oriental, Tokyo, Japan) were continuously available.

2.4. Experimental protocol

2.4.1. Cell proliferation analysis

For assessment of cell proliferation *in vivo*, 5-bromo-2′-deoxyuridine (BrdU 200 mg/kg, Sigma–Aldrich) was administered intraperitoneally when mice reached to 12 weeks of age. After 24 h the four groups of mice were anaesthetized deeply with pentobarbital sodium (50 mg/kg) and fixed by transcardial perfusion with 4% paraformaldehyde. Then the brain was removed and postfixed for 24 h by immersion in 4% paraformaldehyde. Eight coronal slices 1 mm in thickness were made from the fixed forebrain using a rodent brain slicer (Acrylic Matrices, Alto, USA). Serial sections 20 μm in thickness were prepared from each slice with a vibratome (Leica, Wetzlar, Germany). Sections were subjected to double-labeling fluorescence immunohistochemistry with antibody to polysialylated neuronal cell adhesion molecule (PSA-NCAM, Chemicon International) as a marker of migrating neuronal progenitor cells (NPCs), and an antibody to BrdU (Boehringer Ingelheim, Mannheim, Germany).

Cells staining for both BrdU and PSA-NCAM according to confocal microscopy (Olympus, Tokyo Japan) were counted per high-power field (40× objective lens) as newly generated/proliferating neurons. For quantitative analysis, sections including the dentate gyrus of the hippocampus were stained, and BrdU/PSA-NCAM-positive cells in this granule cell layer were counted by two investigators blinded to the experimental protocol. The cell counted then was expressed as cells per millimetre of dentate gyrus. Cells in cerebral cortex stained for both BrdU and PSA-NCAM were counted in 10 fields of cingulate cortex, and the number of positive neocortical cells was expressed as cells per square millimetre.

3. Results

3.1. Behavioural data

3.1.1. Body weight change

Fig. 1 shows body weight change in the four groups of mice during the 8-week housing period. Mixed-type ANOVA indicated no significant main effect of group (G) [$F(3, 40) = 1.486$], while main effect of week (W) and interaction between G and W were significant [$F(7, 280) = 658.43$, $p < .0001$ and $F(21, 280) = 4.746$, $p < .0001$, respectively].

3.1.2. Open-field activity

Fig. 2 shows open-field performance and number of stools after 20 min. Fig. 2A indicates animal locomotion per 1-min block measured by mean number of beam crossing when two beams in each direction were positioned in 10-cm apart. The first 10 min was conducted in light, with the next 10 min in darkness. In general, crossing decreased as time passed during both lighting conditions. Mixed-type ANOVA including one between (group G) and two within-subject factors [light versus dark period (LD), and time in the session (T)] indicated that the main effect of T was significant [$F(9, 360) = 13.865$, $p < .0001$]. Interaction effects of T × G and LD × T were significant [$F(27, 360) = 1.949$, $p = .0037$ and $F(9, 360) = 7.517$, $p < .0001$, respectively]. However, main effects of G and LD and other interaction effects were not significant.

Fig. 2B presents mean number of rearing responses by 1-min block, measured as mean number of horizontal interruptions at 5 cm above the box floor. Mixed-type ANOVA showed that main effects of G, LD, and T all were significant [$F(3, 40) = 3.876$,

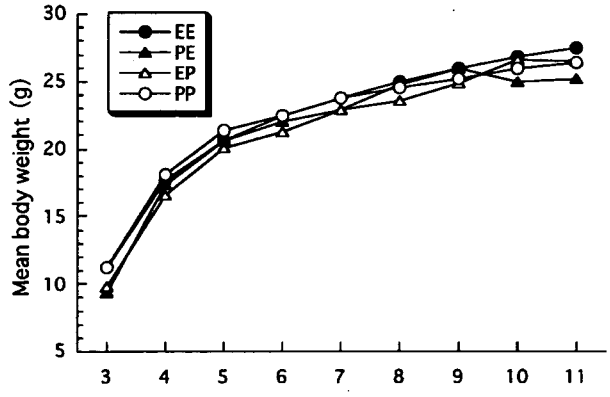

Fig. 1. Mean body weight change of four different housing groups from 3 to 11 weeks of age. Water and food were always available.

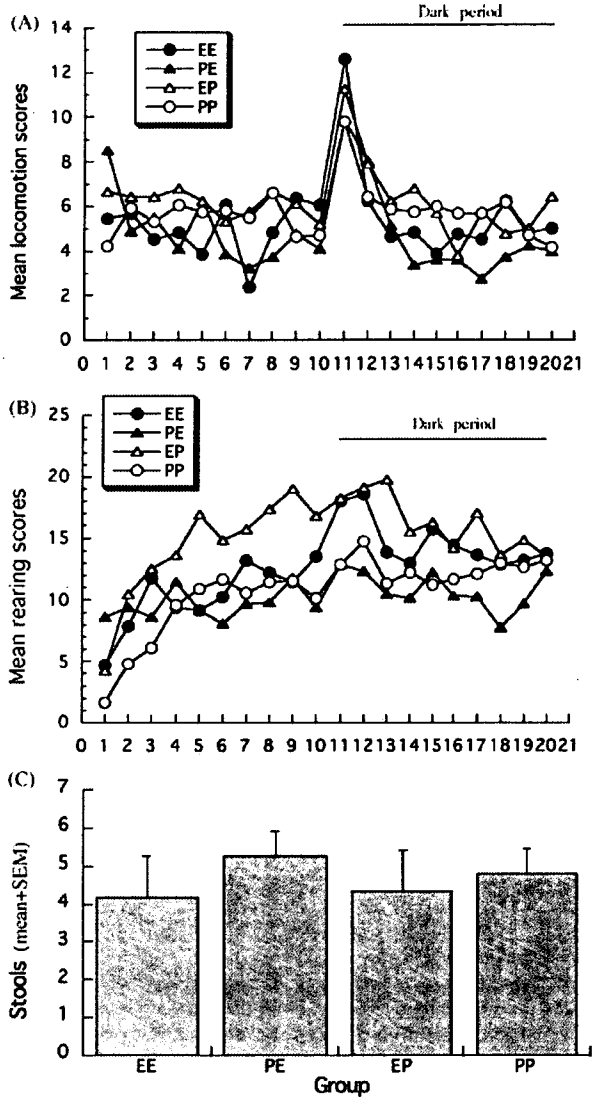

Fig. 2. Results of open-field test. Locomotion (A) counted by horizontal beam-cutting and rearing (B) measured by vertical beam-cutting were plotted. Ten minutes of light period were followed by 10 min of darkness, continuously. Stools found at the end of the session also were counted (C). All data are mean.

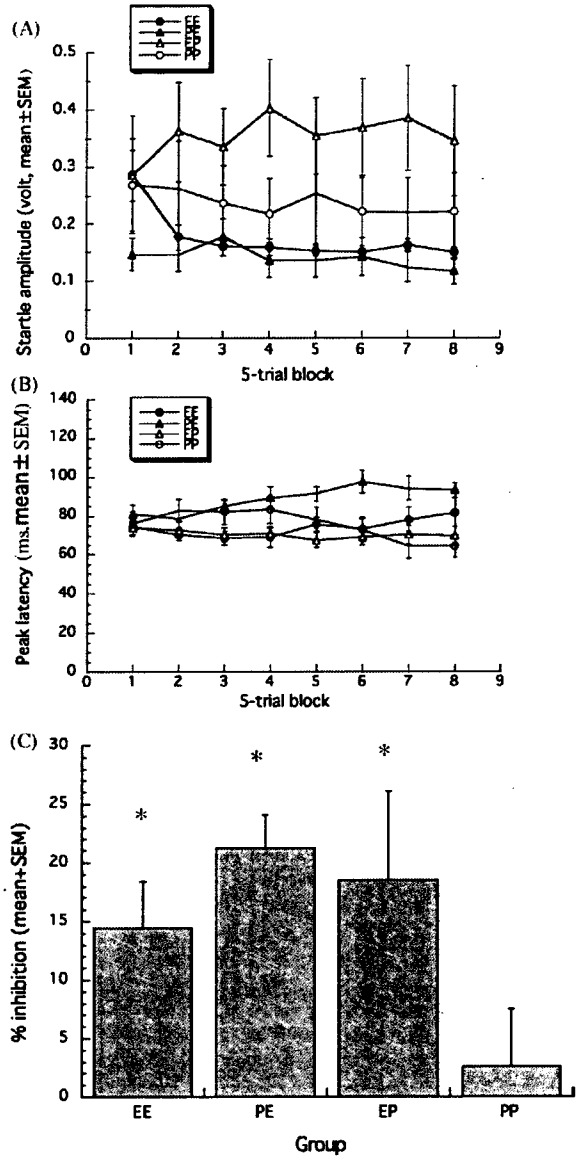

Fig. 3. Results for acoustic startle reflex and prepulse inhibition tests. Startle amplitude in volts (A), and peak latency during 40 trials of habituation (B) were plotted by 5-trial block, and prepulse inhibition by auditory prepulse with 50 ms of lead time (prepulse-pulse interval) condition (C) are shown. Asterisk shows significant inhibition. Data are mean ± SEM.

$p = .0159$; $F(1, 40) = 47.981$, $p < .0001$; $F(9, 360) = 3.682$, $p = .0002$, respectively]. Interaction effects of LD × G, T × G, LD × T, and LD × T × G were significant [$F(3, 40) = 2.937$, $p = .0448$; $F(27, 360) = 1.537$, $p = .0448$; $F(9, 360) = 17.048$, $p < .0001$; $F(27, 360) = 1.803$, $p = .0094$, respectively]. The group differences between EE and EP, EE and PE, EP and PE, and EP and PP were significant by the post hoc test.

Fig. 2C shows the mean number of stools per 20-min session. No group differences were observed [$F(3, 40) < 1$].

3.1.3. Startle reflex and prepulse inhibition

Fig. 3A shows mean amplitude of the auditory startle reflex in the 40 trials of the habituation period by 5-trial block. The results of mixed-type ANOVA indicated no main effects and the interaction effect were significant. Fig. 3B indicates mean peak latencies of the auditory startle reflex. Time to maximum movement amplitude in milliseconds after the start of the startle stimulus was recorded. Group EP showed shorter latency and group PE showed longer latency than the other groups. The results of the mixed-type ANOVA indicated that main effect of G and trial block (TB) [$F(3, 40) = 3.806$, $p = .0172$ and $F(7, 280) = 2.43$, $p = .0197$, respectively] and interactions of TB × G was significant [$F(21, 280) = 1.655$, $p = .0376$]. Fig. 3C shows mean percentage of prepulse inhibition under the auditory prepulse condition at a lead time of 50 ms, in which greatest inhibition was observed. Prepulse inhibition was smallest in the PP group, and inhibitions of the EE, PE and EP groups were significant ($Z = 3.48$, 2.43, and 6.92, respectively), but inhibition of PP mice was not ($Z = 0.53$).

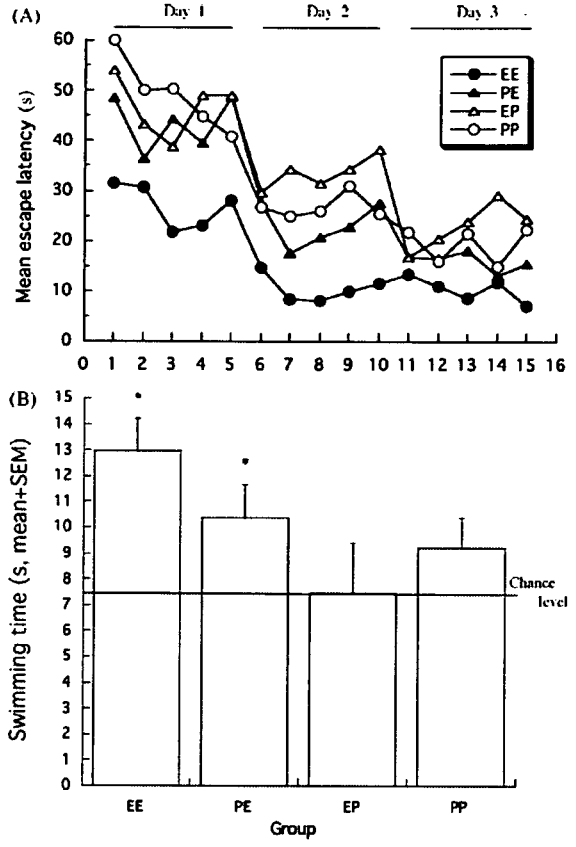

Fig. 4. Results for Morris water-maze learning. Mean latency of all trials in the three daily 5-trial sessions was plotted (A). The differences between EE and the other 3 groups, between PE and EP groups were significant. The results of probe test (B). Mice were allowed to search platform for 30 s. The mean of the total swimming time in the quadrant in which ever had contained the platform during training is shown. Asterisk shows significantly longer swimming time than chance level (7.5 s).

3.1.4. Water-maze learning

Fig. 4A shows mean water-maze latencies for all trials during three daily training sessions. From the first trial, EE mice performed better than other groups, reaching a plateau on the second training day. PP animals performed worst. The PE group showed learning curve intermediate between EE and PP groups. Results of mixed-type ANOVA including one between-subject factor (G) and two within-subject factors (day, D; trial, T) for water-maze learning showed that main effect of G and D were significant [$F(3, 40) = 7.637$, $p = .0004$ and $F(2, 80) = 65.883$, $p < .0001$, respectively]. Main effects of T [$F(4, 160) = 1.764$] and other interaction effects were not significant. The results of post hoc tests indicated group differences between EE and EP, EE and PE, EE and PP, and EP and PE were significant. Fig. 4B shows mean swimming time during 30 s probe test in the quadrant where the platform was placed during water-maze learning. Groups EE and PE showed significantly longer swimming time than the chance level (7.5 s) [$Z = 4.409$, $p < .01$ and $Z = 2.875$, $p < .01$, respectively], but the swimming time of groups PP and EP were not significantly different from the chance level [$Z = .03$ and 1.496, respectively]. Groups EE and PE were better at maze learning than the other two groups,

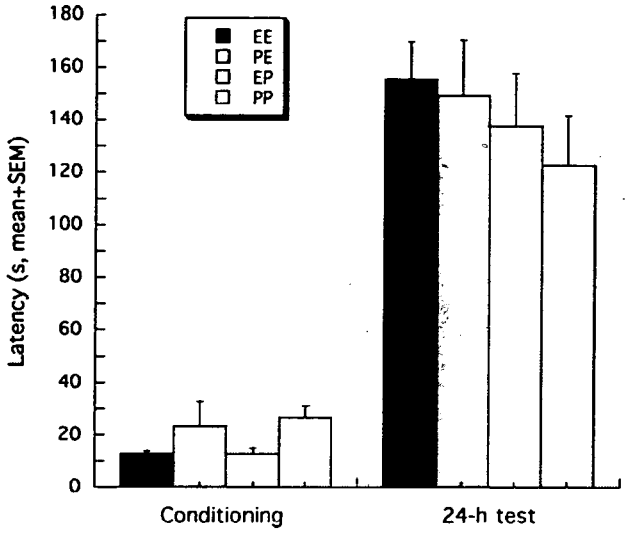

Fig. 5. The results of passive avoidance test. Step-through latencies from light to dark compartments in the conditioning trial (left) and the 24-h test trial (right) are plotted (mean + S.E.M.).

and memorized relatively well where the platform had been placed.

3.1.5. Passive avoidance

Fig. 5 shows mean step-through latencies in the conditioning and 24-h test trials of the passive avoidance test. Although PP mice showed longer latency than EE and EP groups during the conditioning trial, ANOVA performed including the respective trials indicated no group differences for conditioning or 24-h test trials [$F(3, 40) = 2.599$, $p = .065$ and $F(3, 40) < 1$, respectively].

3.2. Neuroanatomic data

3.2.1. Brain weight

Environmental change affected brain weight as well as behaviour. Fig. 6 shows mean weight of the brain determined after completion of all behavioural tests. Animals were 13 weeks old. EE and PE mice had heavier brains than PP and EP animals. ANOVA showed this group effect to be significant [$F(3, 34) = 3.288$, $p < .0323$]. Results of the group comparisons by post hoc tests indicated that group differences between EE and EP, EP and PE, and PE and PP were significant.

3.2.2. Induction of neuronal regeneration in situ

To examine the basis for increased brain weight in the enriched condition, generation of neuronal cells in cerebral cortex and hippocampus was assessed by *in vivo* BrdU labeling. Sections were visualised by confocal microscopy with antibody labeling for BrdU and PSA-NCAM. Cellular profiles for both markers were considered newly generated neurons (Fig. 7). Neuronal generation continued during the enriched condition, but decreased after 2 weeks in the impoverished condition. Newly generated neurons were present at a constant but low level in continuously impoverished (PP) mice.

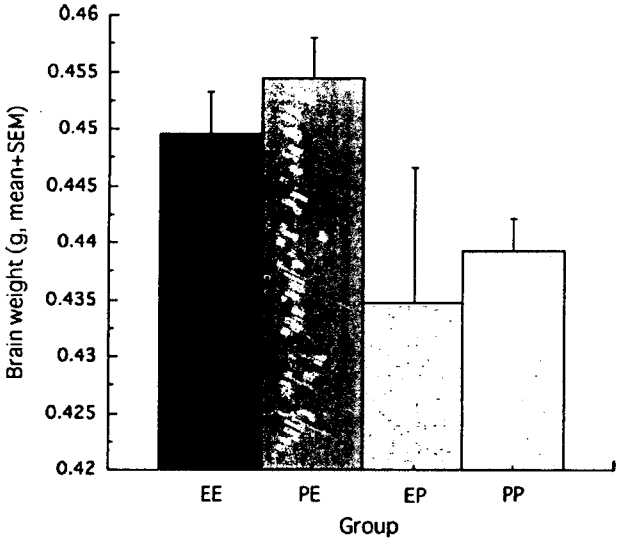

Fig. 6. Brain weight of four groups of mice. Brain was removed and weighted at the next day of the passive avoidance test (13 weeks old) (mean + S.E.M.).

Fig. 8 shows numbers of neurons stained for BrdU in hippocampus (A) and cerebral cortex (B). Neurons were counted in 10 sections for each animal, and were averaged. ANOVA including data for the hippocampus indicated the effect of group to be significant [$F(3, 24) = 8.516$, $p = .0005$]. Post hoc tests showed that group differences between EE and EP, EE and PP, EP and PE, and PE and PP were significant. Thus, environmental enrichment benefited generation of hippocampal neurons, with the most recent environment being critical. PE mice produced more new neurons in the hippocampus than EP mice. Next, ANOVA including data of the cerebral cortex also indicated that the effect of group was significant [$F(3, 25) = 3.169$, $p = .0418$]. Post hoc tests suggested that group differences between EE and EP, EP and PE, and EP and PP groups were significant.

Neurons thus began to increase significantly within 2 weeks after beginning of exposure to the enriched condition. Even a short period of enrichment augmented neuronal proliferation.

4. Discussion

Results of the present experiments reconfirmed that environmental enrichment between weaning and adult had affected development and function of the mouse brain. The brain was

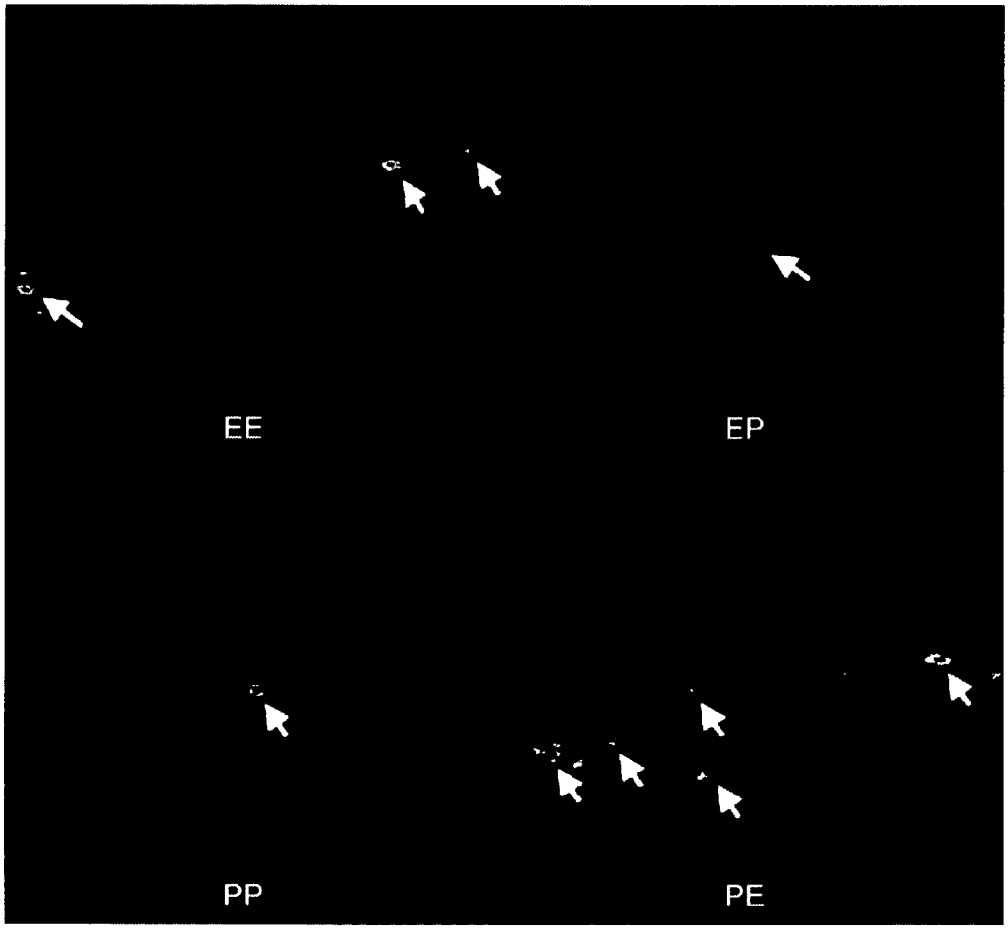

Fig. 7. Newly generated neurons in the hippocampus (arrows). Sections were visualized by confocal microscopy with antibody labeling for BrdU and PSA-NCAM. One example is presented for each group. Original magnification: 200×.

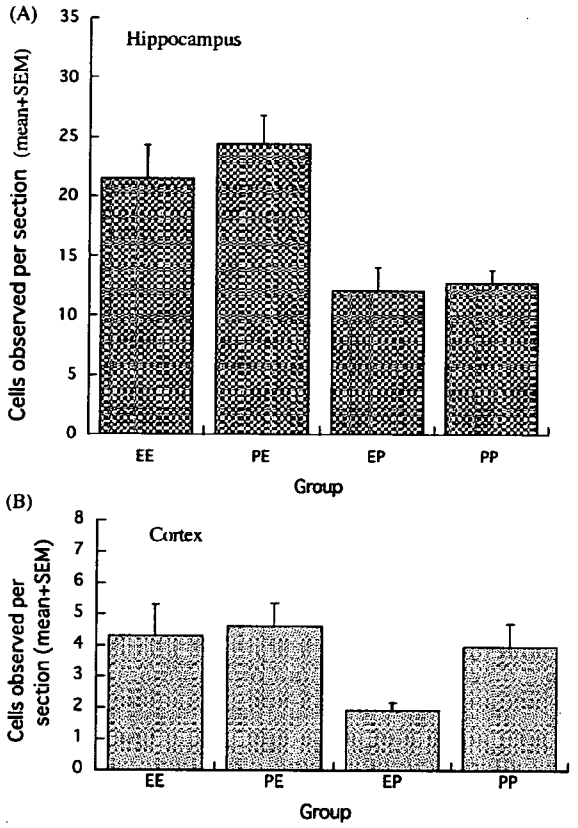

Fig. 8. Newly generated neurons in hippocampus (A) and cerebral cortex (B) per section (mean + S.E.M.). The two groups experienced enrichment during last 2 weeks (EE, PE) showed significantly more neurons labeled by BrdU than the two groups experienced impoverishment during last 2 weeks (EP, PP) in hippocampus. Group EP generated new neurons significantly less than the other three groups in cortex.

heavier in the EE group than the PP group, as in early studies [38,40]. Greater locomotive activities of the PP animals in the open-field test [10,33,41] and smaller prepulse inhibition in the PP mice than EE animals [6] were same as results reported in previous studies. Superior learning in EE mice compared with PP animals also agreed with results of earlier studies [11,29,50].

Moreover, results in the two environment exchange groups indicated that the effect of environment was determined by the most recent condition, suggesting that the plasticity or reorganisation of the brain could take place within a few weeks, even in adult mice. Behavioural results for PE mice resembled to the EE in open-field activity, startle amplitude, water-maze performance, and the probe test; brain weight also was greatest. Some researchers have reported that early impoverishment induced severe and irreversible deficiency in the rats' brain [9,13,51]. Or, development of the brain was not altered by impoverishment, once rats had experienced enrichment [19]. Our results of mice disagreed, the PE group, exposed to an impoverished environment in early life showed superior behavioural performance and heavier brains than the EP group exposed to an enriched environment during early life.

Indirect evidence has accumulated suggesting nervous tissue generation during enrichment [22,23,29,30], an effect also reported after running exercise [47,48]. We therefore expected that neurons would be generated during enriched experience in adult animals even over a short period. Indeed, long-term enrichment was found to increase hippocampal neurons in adult mice [20,21]. Our results in the PE and EP groups were critical in addressing this issue. The PE group generated many neurons in the hippocampus and cerebral cortex after a 2-week experience of enrichment, while results in the EP group suggested the beneficial effects of enrichment early in life could be nullified by impoverishment of conditions for 2 weeks, even in adult mice. Behavioural measures agreed with the anatomic data. PE mice performed better than EP animals, resembling the EE group. The present results that even a short period of enrichment promoted nerve cell generation with behavioural improvement, while a short period of impoverishment induced poor anatomic and behavioural outcomes, suggested that housing conditions are very important for reliable behavioural evaluation of experimental animals. Even "knockedout" mice missing a neurologically important gene reportedly recovered learning and memory after enrichment [8,35]. The results in this area of researches are almost always put in the context of enrichment [20,21,29,38–40]. However, the present results of the EP and PE groups suggest that it is important to study the effects of impoverishment as equally as enrichment. Standardization of housing conditions thus may be unexpectedly important in behavioural neuroscience.

We developed a speculative hypothesis concerning neuronal generation during enriched housing. After observing animals' behaviour in their home cages, enriched and impoverished animals lived completely differently. Enriched animals showed many types of movement, including running, chasing, crouching and fighting, hiding, climbing and wheel-running, and established social order among cage mates. These activities might activate neurons in specific areas of the brain such as hippocampus, cerebral cortex, hypothalamus, visual and motor areas and cerebellum. On the other hand, impoverished mice seldom moved, with less brain activation as a likely consequence. Activation of neurons could induce neurochemical excitation with an increase in regional cerebral blood flow as shown by functional magnetic resonance imaging (fMRI). Recent findings have shown neuronal regeneration after cerebral ischemia [3,28], regeneration was promoted if blood flow in ischemic brain was restored by angiogenesis [45]. Mechanisms underlying such effects are unclear, but recovery of blood flow might accelerate removal of debris or toxic products from the injured brain, and/or enhance production of chemokines and trophic agents [23,30]. If this hypothesis is true, neuron genesis and functional enhancement by enrichment in young adult mice might arise from brain stimulation and remodeling of blood flow. Our findings showed that an enriched environment enhanced neuron genesis in the mouse hippocampus and cingulated cortex, both of which participate in memory function. On the other hand, impoverished environment impaired neuron genesis. Based on these data, enriched experience appears to be essential for enhancing endogenous neuron genesis and improving functional recovery.

Recent animal welfare movement has advocated important of housing and care for laboratory rodents, giving animals greater

opportunity to carry out species-specific behavioural repertoires [4,18]. To answer the demand for standardized of environmental enrichment for laboratory animals, increasing numbers of rodent care products are coming available, even accommodating differences in preference for nest boxes in mice [46]. Improvements in housing conditions are expected to cause some discrepancies between early and present data, not only in behavioural observations but also for other biologic characteristics.

Finally, environmental enrichment has been used to promote the mental health of persons at risk [36,37]. For example, Rane et al. [36] assessed the effect of environmental enrichment including nutrition, education, and physical exercise at ages from 3 to 5 years in children with risk factors for later emergence of schizophrenia. Schizotypical personality features and antisocial behaviour were assessed at the ages of 17 and 23 years. Results suggested that the early enrichment program was effective; subjects who participated had more normal scores upon assessment in adolescence than untreated at-risk controls. These results are consistent with animal studies in which an enriched environment benefited behavioural and biologic outcomes. Moreover, our finding that even a short period of environmental enrichment positively affected behaviour and generation of neurons in the adult mouse suggested that even adults and elderly persons could benefit from enrichment, improving cognitive and memory functions. On the other hand, hospitalization or isolation might cause deterioration even in adults. Although the present experiment could not differentiate physical and social environments as the factor to influence the present results, we would like to testify whether social or physical, or the combination of both factors, cause the present effects in the future study.

Acknowledgments

This work was partially supported by a Grant-in Aid for Scientific Research (C) No. 17530540 in the Japanese Ministry of Education, Science, Sports and Culture and by a Research Grant for Cardiovascular Diseases. We would like to thank Ms. Yuka Okinaka for technical assistance.

References

[1] Akita H, Matsuyama T, Iso H, Sugita M, Yoshida S. Effects of oxidative stress on the expression of limbic-specific protease neuropsin and avoidance learning in mice. Brain Res 1997;967:86–96.
[2] Altman JA, Das GD. Autoradiographic examination of the effects of enriched environment on the rate of glial multiplication in the adult rat brain. Nature 1964:1161–3.
[3] Arvidsson A, Collin T, Kirik D, Kokaia Z, Lindvall O. Neuronal replacement from endogenous precursors in the adult brain after stroke. Nat Med 2002;8:963–70.
[4] Baumans V. Environmental enrichment for laboratory rodents and rabbits: requirements of rodents, rabbits, and research. ILAR J 2005;46:162–70.
[5] Benaroya-Milshtein N, Hollander N, Apter A, Kukulansky T, Raz N, Wilf A, et al. Environmental enrichment in mice decreases anxiety, attenuates stress responses and enhances natural killer cell activity. Eur J Neurosci 2004;20:1341–7.
[6] Cilia J, Reavill C, Hagan JJ, Jones DNC. Long-term evaluation of isolation-rearing induced prepulse inhibition deficits in rats. Psychopharmacology 2001;156:327–37.
[7] Dannis C. All in the mind of a mouse. Nature 2005;438:151–2.
[8] Duffy SN, Craddock KJ, Abel T, Nguyen PV. Environmental enrichment modifies the PKA-dependence of hippocampal LTP and improves hippocampus-dependent memory. Learn Memory 2001;8:26–34.
[9] Einon DF, Morgan MJ. A critical period for social isolation in the rat. Dev Psychobiol 1977;10:123–32.
[10] Elliott BM, Grunberg NE. Effects of social and physical enrichment on open field activity differ in male and female Sprague–Dawley rats. Behav Brain Res 2005;165:187–96.
[11] Ferchmin PA, Eterovic VA. Forty minutes of experience increase the weight and RNA content of cerebral cortex in periadolescent rats. Dev Psychobiol 1986;19:511–9.
[12] Ferchmin PA, Eterovic VA, Caputto R. Studies of brain weight and RNA content after short periods of exposure to environmental complexity. Brain Res 1970;20:49–57.
[13] File SE. Exploration, distraction, and habituation in rats reared in isolation. Dev Psychobiol 1978;11:73–81.
[14] Gentch C, Lichtsteiner M, Frischnecht HR, Feer H, Siegfried B. Isolation-induced locomotor hyper-activity and hypoanalgesia in rats are prevented by handling and reversed by resocialisation. Physiol Behav 1988;43:13–6.
[15] Gobbo OL, O'Mara SM. Impact of enriched-environment housing on brain-derived neurotrophic factor and on cognitive performance after a transient global ischemia. Behav Brain Res 2004;152:231–41.
[16] Gottleb G, Blair C. How early experience matters in intellectual development in the case of poverty. Prevent Sci 2004;5:245–52.
[17] Huck UW, Price EO. Differential effects of environmental enrichment on the open-field behavior of wild and domestic Norway rats. J Comp Physiol Psychol 1975;89:892–8.
[18] Hutchinson E, Avery A, Vandewoude S. Environmental enrichment for laboratory rodents. ILAR J 2005;46:148–61.
[19] Katz HB, Davies CA. Effects of differential environments on the cerebral anatomy of rats as a function of previous and subsequent housing conditions. Exp Neurol 1984;83:274–87.
[20] Kempermann G, Brandon EP, Gage FH. Environmental stimulation of 129/SvJ mice causes increased cell proliferation and neurogenesis in the adult dentate gyrus. Curr Biol 1998.
[21] Kempermann G, Kuhn HG, Gage FH. More hippocampal neurons in adult mice living in an enriched environment. Nature 1997;386:493–5.
[22] Leggio MG, Mandolesi L, Federico F, Spirito F, Ricci B, Gelfo F, et al. Environmental enrichment promotes improved spatial abilities and enhanced dendritic growth in the rat. Behav Brain Res 2005;163:78–90.
[23] Lewis MH. Environmental complexity and central nervous system development and function. Mental Retard Dev Disabil Rev 2004;10:91–5.
[24] Lodge DJ, Lawrence AJ. The effect of isolation rearing on volitional ethanol consumption and central CCK/dopamine systems in Fawn-Hooded rats. Behav Brain Res 2003;141:113–22.
[25] Matsuyama S, Doe N, Kurihara N, Tanizawa K, Kuroda S, Iso H, et al. Spatial learning of mice lacking a neuron-specific epidermal growth factor family protein, NELL2. J Pharmacol Sci 2005;98:239–43.
[26] McIlwain KL, Merriweather MY, Yuva-Paylor LA, Paylor R. The use of behavioral test batteries: effects of training history. Physiol Behav 2001;73:705–17.
[27] Morgan MJ. Effects of post-weaning environment on learning in the rat. Anim Behav 1973;21:429–42.
[28] Nakatomi H, Kuriu T, Okabe S, Yamamoto S, Hatano O, Kawahara N, et al. Regeneration of hippocampal pyramidal neurons after ischemic brain injury by recruitment of endogenous neural progenitors. Cell 2002;110:429–41.
[29] Pham TM, Soderstrom S, Winblad B, Mohammed AH. Effects of environmental enrichment on cognitive function and hippocampal NGF in the non-handled rats. Behav Brain Res 1999;103:63–70.
[30] Pham TM, Winblad B, Granholm A, Mohammed AH. Environmental influences on brain neurotrophines in rats. Pharmacol Biochem Behav 2002;73:167–75.
[31] Phillips GD, Howes SR, Whitelaw RB, Robbins TW, Everitt BJ. Isolation rearing impairs the reinforcing efficacy of intravenous cocaine or intra-accumbens D-amphetamine: impaired response to intra-accumbens D1 and D2/D3 dopamine receptor antagonists. Psychopharmacology 1994;115:419–29.

[32] Phillips GD, Howes SR, Whitelaw RB, Wilkinson LS, Robbins TW, Everitt BJ. Isolation rearing enhances the locomotor response to cocaine and a novel environment, but impairs the intravenous self-administration of cocaine. Psychopharmacology 1994;115:407–18.
[33] Pietropaolo S, Branchi I, Cirulli F, Chiarotti F, Aloe L, Alleva E. Long-term effects of the periadolescent environment on exploratory activity and aggressive behaviour in mice: social versus physical enrichment. Physiol Behav 2004;81:443–53.
[34] Pryce CR, Bettschen D, Nanz-Bahr NI, Feldon J. Comparison of the effects of early handling and early deprivation on conditioned stimulus, context, and spatial learning and memory in adult rats. Behav Neurosci 2003;117:883–93.
[35] Rampon C, Tang Ya-P, Goodhouse J, Shimizu E, Kyin M, Tsien JZ. Enrichment induces structural changes and recovery from nonspatial memory deficit in CA1 NMDAR1-knockout mice. Nat Neurosci 2000;3:238–45.
[36] Rane A, Mellingen K, Liu J, Vanables PH, Mednick SA. Effects of environmental enrichment at ages 3–5 years on schizotypical personality and antisocial behavior at ages 17 and 23 years. Am J Psychiatry 2003;160:1627–35.
[37] Rane A, Vanables PH, Dalais C, Mellingen K, Reynolds C, Mednick SA. Early educational and health enrichment at age 3–5 years is associated with increased autonomic and central nervous system arousal and orienting at age 11 years: evidence from Mauritius Child Health Project. Psychophysiology 2001;38:254–66.
[38] Rosenzweig MR. Environmental complexity, cerebral change, and behavior. Am Psychol 1966;21:321–32.
[39] Rosenzweig MR, Bennett EL. Psychobiology of plasticity: effects of training and experience on brain and behavior. Behav Brain Res 1996;78:57–65.
[40] Rosenzweig MR, Krech D, Bennett EL, Diamond MC. Effects of environmental complexity and training on brain chemistry and anatomy: a replication and extension. J Comp Physiol Psychol 1962;55:429–37.
[41] Sahakian BJ, Robbins TW, Morgan MJ, Iversen SD. The effects of psychomotor stimulants on stereotypy and locomotor activity in socially-deprived and control rats. Brain Res 1975;84:195–205.
[42] Sasaki H, Iso H, Coffey P, Inoue T, Fukuda Y. Prepulse facilitation of auditory startle response in hamsters. Neurosci Lett 1998;248:117–20.
[43] Seki T, Arai Y. The persistent expression of a highly polysialylated NCAM in the dentate gyrus of the adult rat. Neurosci Res 1991;12:503–13.
[44] Seki T, Arai Y. Highly polysialylated neural cell adhesion molecule (NCAM) is expressed by newly generated granule cells in the dentate gyrus of the adult rat. J Neurosci 1993;13:2351–8.
[45] Taguchi A, Soma T, Tanaka H, Kanda T, Nishimura H, Yoshikawa H, et al. Administration of CD34+ cells after stroke enhances neurogenesis via angiogenesis in a mouse model. J Clin Invest 2004;114:330–8.
[46] Van Loo PL, Bloom HJ, Meijer MK, Baumans V. Assessment of the use of two commercially available environmental enrichments by laboratory mice by preference testing. Lab Anim 2005;39:58–67.
[47] Van Praag H, Cristie BR, Sejnowski TJ, Gage FH. Running enhances neurogenesis, learning and long-term potentiation in mice. Proc Natl Acad Sci USA 1999;96:13427–31.
[48] Van Praag H, Kempermann G, Gage FH. Running increases cell proliferation and neurogenesis in the adult mouse dentate gyrus. Nat Neurosci 1999;2:266–70.
[49] Van Praag H, Kempermann G, Gage FH. Neural consequences of environmental enrichment. Nat Rev Neurosci 2000;1:191–8.
[50] Wood WE, Greenough WT. Effect of grouping and crowding on learning in isolation-reared adult rats. Bull Psychon Soc 1974;3:65–7.
[51] Wright IK, Upton N, Marsden CA. Resocialization of isolation-reared rats does not alter their anxiogenic profile on the elevated X-maze model of anxiety. Physiol Behav 1991;50:1129–32.
[52] Yukawa K, Iso H, Tanaka T, Tsubota Y, Owada-Makabe K, Bai T, et al. Down-regulation of dopamine transporter and abnormal behavior in STAT6-deficient mice. Int J Mol Med 2005;15:819–25.
[53] Yukawa K, Tanaka T, Owada-Makabe K, Tsubota Y, Bai T, Maeda M, et al. Reduced prepulse inhibition of startle in STAT6-deficient mice. Int J Mol Med 2005;16:673–5.

ORIGINAL RESEARCH

Visualization of Intracerebral Arteries by Synchrotron Radiation Microangiography

K. Myojin
A. Taguchi
K. Umetani
K. Fukushima
N. Nishiura
T. Matsuyama
H. Kimura
D.M. Stern
Y. Imai
H. Mori

BACKGROUND AND PURPOSE: Small cerebral vessels are a major site for vascular pathology leading to cerebral infarction and hemorrhage. However, such small cerebral vessels are difficult to visualize by using conventional methods. The goal of our study was the development of methodology allowing visualization of small cerebral arteries in rodents, suitable for experimental models.

MATERIALS AND METHODS: Using barium sulfate as a contrast material, we obtained microangiographic images of physiologic and pathologic changes consequent to cerebral infarction in mouse brain by monochromatic synchrotron radiation (SR). To achieve high-resolution and high-contrast images, we used a new x-ray camera with a pixel size of 4.5 μm, and we set the energy level at 37.5 keV, just above the K absorption of barium.

RESULTS: Small intracerebral arteries (~30 μm in diameter) were clearly visualized, as well as the cortical branches (50–70 μm in diameter) at the brain surface. The limit of detection appeared to be vessels ~10 μm in diameter. Compared with the noninfarcted side, the number of intracerebral arteries was dramatically decreased in the middle cerebral artery area affected by stroke.

CONCLUSIONS: These results indicate the potential of SR for evaluating pathologic changes in small cerebral arteries and for monitoring the impact of pro- and antiangiogenic therapeutic strategies.

Cerebrovascular disease is one of the major causes of death and disability in developed countries. To evaluate cerebral vasculature, conventional angiography and MR angiography are commonly used in clinical practice. The development of these imaging methods has allowed analysis of the pathologic features of cerebrovascular lesions and has guided therapeutic strategies. However, small cerebral vessels, including those known to harbor causative lesions in cerebral infarction and hemorrhage (due to lipohyalinotic changes and/or microaneurysm formation),[1] such as intracerebral arteries and perforators, are below the detection limit of conventional imaging techniques. An important step in developing therapeutic strategies effective against disease in small cerebral vessels is enhanced visualization of this vasculature, especially in experimental models.

Recently, ex vivo and in vivo microangiography using monochromatic synchrotron radiation (SR) has been suggested as a tool capable of visualizing pathophysiologic changes in small arteries. Using this system has made possible the detection of microcirculation in the dermis,[2] tumors,[3] and collateral microvessels in ischemic hind limbs.[4] Although fluorescence microscopy has also been used to image small arteries,[5-7] SR imaging has the advantage of visualizing microvessels, even after they enter the parenchyma of an organ. In contrast, fluorescence techniques do not allow adequate visualization of small arteries once a vessel is deep within brain or other parenchymal tissue. On the basis of these observations, we have developed a microangiographic system using SR and have investigated physiologic and pathologic features of rodent cerebral microvasculature.

Received August 3, 2006; accepted after revision August 31.

From the Departments of Cerebrovascular Disease (K.M., A.T.) and Cardiac Physiology (K.F., N.N., H.M.), National Cardiovascular Center, Osaka, Japan; the Department of Radiology (K.M., Y.I.), Tokai University School of Medicine, Kanagawa, Japan; Japan Synchrotron Radiation Research Institute (K.U.), Hyogo, Japan; the Department of Internal Medicine (T.M.), Hyogo College of Medicine, Hyogo, Japan; Dainippon Sumitomo Pharma Co Ltd (H.K.), Osaka, Japan; and the Dean's Office (D.M.S.), College of Medicine, Cincinnati University, Cincinnati, Ohio.

Experiments were performed at the SPring-8 BL28B2 beamline with the approval of the Japan Synchrotron Radiation Research Institute (acceptance No. 2005B0358).

This work was partially supported by a Grant-in-Aid for Scientific Research from the Ministry of Health, Labor and Welfare and The New Energy and Industrial Technology Development Organization.

Please address correspondence to Akihiko Taguchi, MD, Department of Cerebrovascular Disease, National Cardiovascular Center, 5-7-1 Fujishiro-dai, Suita, Osaka, Japan, 565-8565; e-mail: Taguchi ataguchi@res.ncvc.go.jp

Materials and Methods

All procedures were performed in accordance with the National Cardiovascular Center Animal Care and Use Committee.

Preparation of Contrast Medium

For high-contrast images of the microcirculation, contrast agents included microspheres (Techpolymer I-2, Sekisui Plastics, Shiga, Japan) and barium sulfate (BarytgenSol, Fushimi, Tokushima, Japan). However, because the diameter of microspheres was 15 μm, whereas that of barium sulfate particles varied from 1–100 μm, the microcirculation of cerebral arteries could not be visualized by using these contrast media (not shown). To perfuse such microvessels (diameter <10 μm), we filtered barium sulfate (pore size 5 μm; Millex-SV, Millipore, Bedford, Mass) and obtained particles <5 μm in diameter. Filtered barium sulfate particles were then centrifuged (3000 G, 60 minutes) and concentrated to 50% by weight following removal of the supernatant.

Injection of Contrast Medium

Male severe combined immunodeficient (SCID) mice (6 weeks old; weight, 25–30 g; Oriental Yeast, Tokyo, Japan) were anesthetized by using inhaled diethyl ether and were perfused systemically with phosphate-buffered saline (PBS) containing heparin (40 U/mL) via the left ventricle of the heart with a peristaltic pump (Iwaki, Asahi Techno Glass, Chiba, Japan). Filtered barium sulfate particles (<5 μm in diameter, prepared as described previously; 50% by weight) were infused (0.7 mL), followed by isolation of the brain and fixation in formalin.

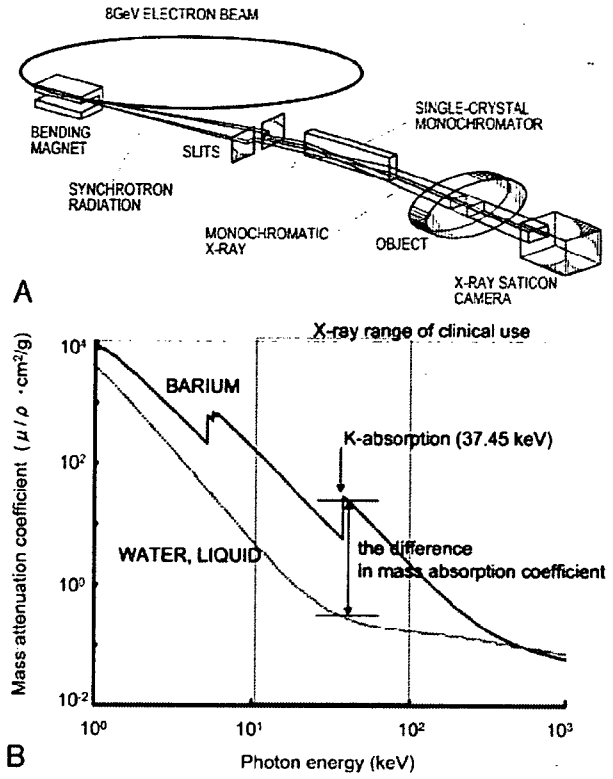

Fig 1. Schematic depiction of the monochromatic SR system. *A*, Illustration of the experimental arrangement for SR microangiography at BL28B2. *B*, Photon mass attenuation coefficient of barium (*blue line*) and liquid water (*red line*). Monochromatic x-ray energy is adjusted to 37.5 keV, just above the barium K-edge energy to produce the highest contrast image.

Microangiography and Image Analysis

Microangiographic images of mouse brain were obtained by using monochromatic SR in the Japan Synchrotron Radiation Research Institute (SPring-8, Hyogo, Japan).[4,8] There are 3 large 3rd-generation synchrotron radiation facilities in the world: the Advanced Photon Source in Argonne (United States), the European Synchrotron Radiation Facility in Grenoble (France), and SPring-8 (the latter was used for the studies described herein). These facilities are open to scientists in many fields, including material, chemical, and life sciences investigators. The experimental setup for x-ray imaging by using monochromatic SR at the SPring-8 BL28B2 beamline is shown in Fig 1*A*. The storage ring was operated at 8-GeV electron beam energy, and beam current was 80–100 mA. The distance between the point source in the bending magnet and the detector was ~45 m. A nearly parallel x-ray beam was used for imaging without blurring because of the small size of the x-ray source and the very long source-to-object distance. The single crystal monochromator selects a single energy of synchrotron radiation. The shutter system is located between the monochromator and the object. X-rays transmitted through the object are detected by an x-ray direct-conversion-type detector incorporating the x-ray saticon pickup tube. Monochromatic x-ray energy was adjusted to 37.5 keV, just above the barium K-edge energy, to produce the highest contrast image of the barium (Fig 1*B*). X-ray flux at the object position was around 1×10^{10} photons/mm^2 per second in imaging experiments. The images were acquired as 1024 × 1024 pixels with 10-bit resolution after analog-to-digital conversion. The FOV was 4.5 × 4.5 mm^2, and pixel size was ~4.5 μm.[9,10]

Mammographic Images

To compare spatial and contrast resolution, we obtained mammographic images, which are known for having the highest resolution in clinical applications,[11] of murine brains. Digital images were captured at an energy level of 24 kV by using a molybdenum target and a molybdenum filter with 90° cranial projection. Source-to-image distance was 65 cm.

Induction of Focal Cerebral Ischemia

Permanent focal cerebral infarction was induced by ligation and disconnection of the left MCA of male SCID mice (n = 5), as described.[12–14] Briefly, under inhaled halothane (3%) anesthesia, animals were placed on their right sides and a skin incision was made at the midpoint between the left orbit and the external auditory canal. The temporalis muscle was incised, and the zygomatic arch was removed to expose the squamous portion of the temporal bone. Using a dental drill, we made a small hole above the distal portion, M1, of the MCA, which could be seen through the exposure in the skull. The dura mater was opened, and the left MCA was electrocauterized and disconnected just distal to its crossing of the olfactory tract. Body temperature was maintained at 36.5°–37°C by using a heat lamp during the operation and for 2 hours after MCA occlusion. Cerebral blood flow (CBF) in the left MCA area was measured by laser-Doppler flowmetry (Advance, Tokyo, Japan). The holding device of the laser probe (ALF probe; Neuroscience, Osaka, Japan) (1.5 mm in diameter, 7.0 mm in length) was secured on the cranium at a site located above the ischemic core of the left MCA area (approximately 1 mm anterior and 5 mm distal to the bregma), and CBF was monitored during the procedure and 24 hours after ligation of the MCA. Mice displaying a decrease in CBF by ~75% immediately after the procedure and thereafter for an additional 24 hours were used for experiments.[15] Nine days after induction of cerebral ischemia, the cerebral microcirculation was examined by SR imaging.

MR Imaging System

To confirm cerebral infarction consequent to ligation of the MCA, we performed MR imaging on day 2 poststroke. MR imaging used a 2T compact MR imaging system with a permanent magnet (MRmini SA206, Dainippon Sumitomo Pharma, Osaka, Japan) by using a radio-frequency solenoid coil for signal-intensity detection. For each imaging sequence, 15 coronal images were acquired with a section thickness of 1 mm, gapped at 0.5 mm. T1-weighted spin-echo MR images were acquired with a TR/TE of 500/9 ms, a FOV of 36.6 × 18.3 mm, an image acquisition matrix of 256 × 128, and NEX, 4. T2-weighted spin-echo MR images were obtained with TR/TE, 3000/69, 256 × 128, and NEX, 2. Because the sequences to obtain diffusion-weighted images by using this machine are still in development, we evaluated the cerebral ischemia by T2-weighted images on day 2 poststroke.

Data Analysis

In all experiments, the mean ± SE is reported.

Results

Visualization of Cerebral Arteries by SR Imaging

After euthanasia and systemic perfusion with PBS, barium sulfate particles were infused via the left ventricle of the heart. As shown in Fig 2*A*, cerebral arteries on the brain surface were filled with contrast medium. First, we investigated vascular

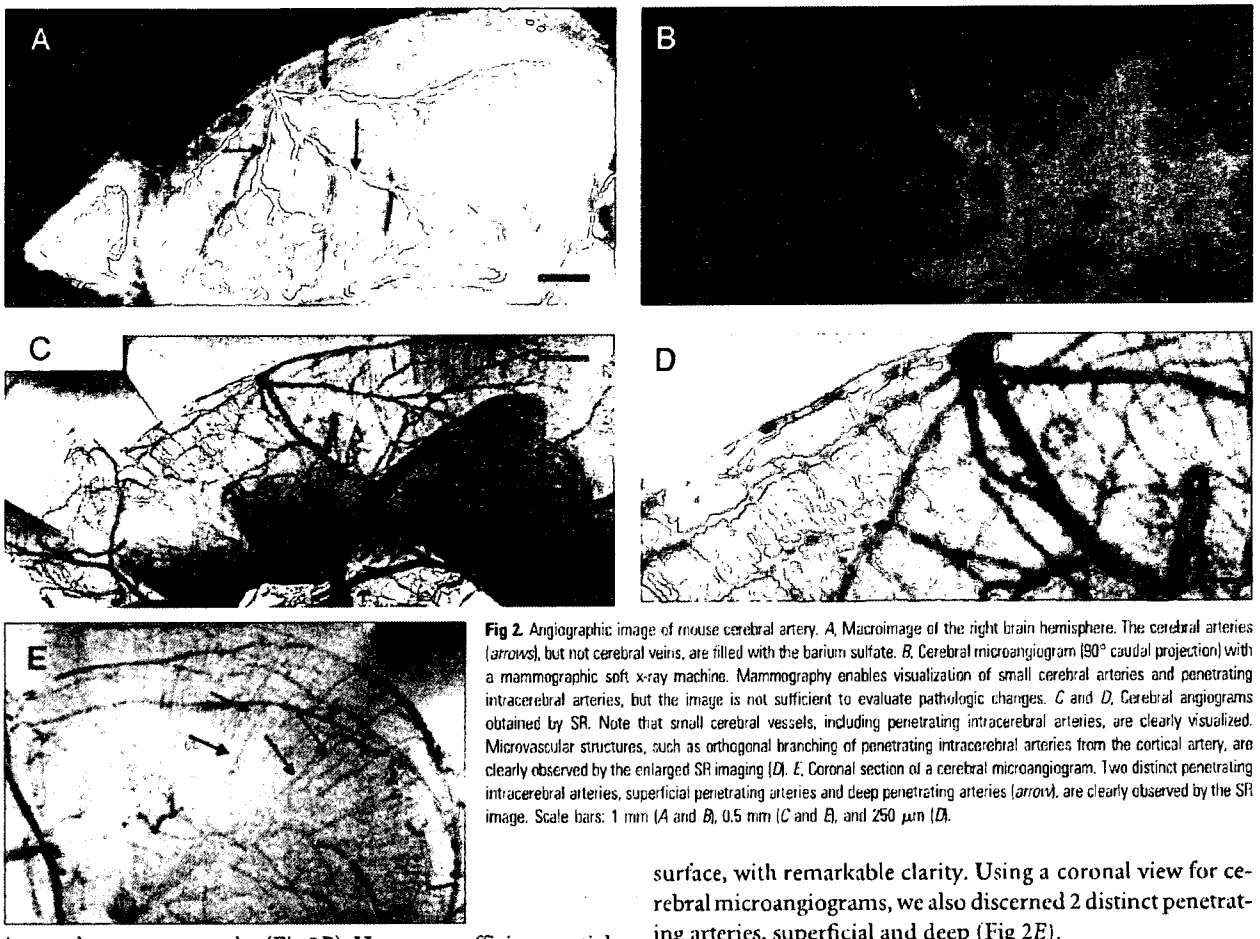

Fig 2. Angiographic image of mouse cerebral artery. *A*, Macroimage of the right brain hemisphere. The cerebral arteries (*arrows*), but not cerebral veins, are filled with the barium sulfate. *B*, Cerebral microangiogram (90° caudal projection) with a mammographic soft x-ray machine. Mammography enables visualization of small cerebral arteries and penetrating intracerebral arteries, but the image is not sufficient to evaluate pathologic changes. *C* and *D*, Cerebral angiograms obtained by SR. Note that small cerebral vessels, including penetrating intracerebral arteries, are clearly visualized. Microvascular structures, such as orthogonal branching of penetrating intracerebral arteries from the cortical artery, are clearly observed by the enlarged SR imaging (*D*). *E*, Coronal section of a cerebral microangiogram. Two distinct penetrating intracerebral arteries, superficial penetrating arteries and deep penetrating arteries (*arrow*), are clearly observed by the SR image. Scale bars: 1 mm (*A* and *B*), 0.5 mm (*C* and *E*), and 250 μm (*D*).

images by mammography (Fig 2*B*). However, sufficient spatial and contrast resolution was not obtained by mammographic imaging to evaluate the angioarchitecture of small cerebral vasculature. Peripheral branches of the MCA (75–100 μm in diameter) and small vessels emerging from peripheral branches were barely visualized.

Next, we investigated the vascular profile by using SR (Fig 2*C*, normal view; -*D*, enlarged view). At the brain surface, cortical arteries branching from the MCA and pial arteries, ~30 μm in diameter, were clearly visualized. Within the brain parenchyma, penetrating intracerebral arteries, branching orthogonally from cortical or pial arteries, were also observed. The interval between intracerebral arteries was 126.1 ± 35.5 μm (n = 20), the diameter of the proximal side of the intracerebral arteries was 29.5 ± 3.1 μm (n = 20), and each intracerebral artery was observed to progressively narrow to a diameter below the limit of resolution (10 μm). Vascular diameters determined by SR imaging of intracerebral arteries and small arterial branches were identical to those observed in previous pathologic studies of murine brain.[16] Using SR imaging, we could discern 2 types of intracerebral arteries: superficial penetrating arteries perfusing only the cortical area and penetrating arteries reaching the subcortical area and perfusing the deep white matter. These vascular structures observed in murine brain by SR imaging are similar to previous observations in human anatomic studies.[17-20] Compared with mammographic images, SR imaging enabled visualization of penetrating intracerebral arteries (diameter range of 10–30 μm), as well as small peripheral branches of MCA at the brain surface, with remarkable clarity. Using a coronal view for cerebral microangiograms, we also discerned 2 distinct penetrating arteries, superficial and deep (Fig 2*E*).

SR Images after Cerebral Infarction

To evaluate cerebral vasculature in the context of pathologic changes, cerebral infarction was induced by ligation of the MCA. The area of cerebral infarction was visualized by MR imaging on day 2 after induction of stroke. As we have shown previously by 2,3,5-triphenyltetrazolium staining,[12] limited cortical infarction was observed in the MCA area on T2-weighted images (Fig 3*A*). In contrast, no hyper- or hypointense region was observed on T1-weighted images (Fig 3*B*), indicating the absence of bleeding or parenchymal injury. Although no morphologic (Fig 3*C*) or vascular structural (Fig 3*D*) changes were observed in the right hemisphere (nonstroke side), by day 9 after MCA occlusion, tissue degradative changes were observed in the cortical and shallow white matter of the left MCA area (stroke side, Fig 3*E*). To evaluate the integrity of the microvasculature after stroke, we obtained SR images. The number of penetrating intracerebral arteries dramatically decreased, though cortical branches at the brain surface could still be visualized (Fig 3*F*). On the coronal view, the disappearance of the intracerebral arteries on the ischemic side was also clearly observed (Fig 3*G*).

Discussion

Cerebral artery disease in small vessels is a major cause of cerebral infarction and hemorrhage. Although pathologic changes in small arteries have been reported on the basis of microscopic analysis, it has been difficult to assess the mor-

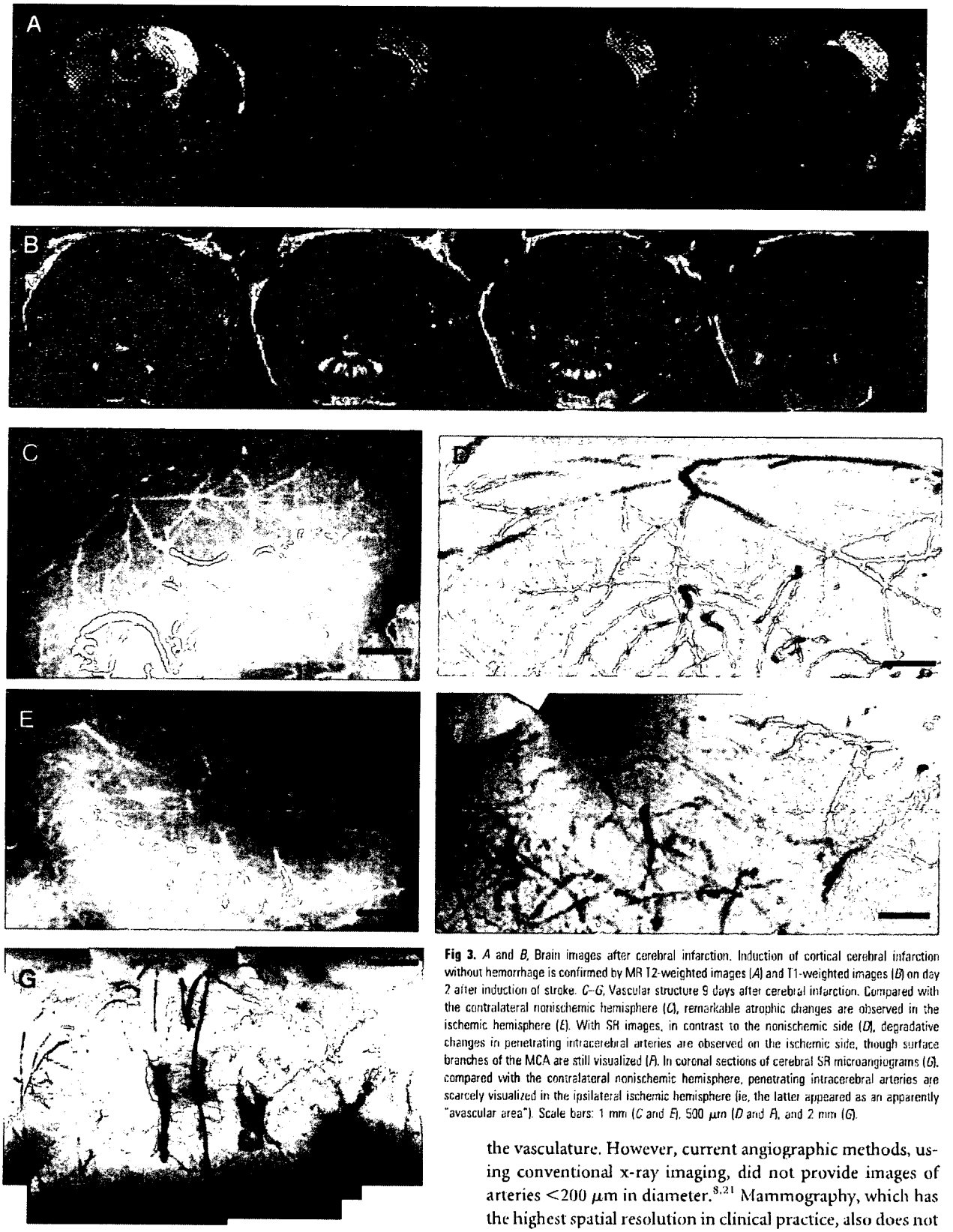

Fig 3. *A* and *B*, Brain images after cerebral infarction. Induction of cortical cerebral infarction without hemorrhage is confirmed by MR T2-weighted images (*A*) and T1-weighted images (*B*) on day 2 after induction of stroke. *C–G*, Vascular structure 9 days after cerebral infarction. Compared with the contralateral nonischemic hemisphere (*C*), remarkable atrophic changes are observed in the ischemic hemisphere (*E*). With SR images, in contrast to the nonischemic side (*D*), degradative changes in penetrating intracerebral arteries are observed on the ischemic side, though surface branches of the MCA are still visualized (*F*). In coronal sections of cerebral SR microangiograms (*G*), compared with the contralateral nonischemic hemisphere, penetrating intracerebral arteries are scarcely visualized in the ipsilateral ischemic hemisphere (ie, the latter appeared as an apparently "avascular area"). Scale bars: 1 mm (*C* and *E*), 500 μm (*D* and *F*), and 2 mm (*G*).

phology of small cerebral vessels in situ through imaging studies. Herein, we demonstrate that small cerebral vessels can be clearly visualized by microangiography by using SR.

Conventional angiography is commonly used to evaluate the vasculature. However, current angiographic methods, using conventional x-ray imaging, did not provide images of arteries <200 μm in diameter.[8,21] Mammography, which has the highest spatial resolution in clinical practice, also does not have sufficient resolution to visualize small vessels with a diameter of <50 μm.[11] Microangiographic techniques have been developed by using fine-focus x-rays and sensitive films to evaluate the microcirculation in the brain.[20] These methods enable visualization of human cortical perforating arteries and

medullary long branches (100 μm in diameter) by using 1-cm-thick sections of brain.[20] However, the limit of detection by using these methods applied to thick sections has been reported to be vessels of 50 μm in diameter.[22] Furthermore, visualization of smaller arteries required thin sections cut with a microtome.[20] The latter method is not well-suited to the evaluation of 3D cerebral vascular trees.

Compared with these conventional methods, the principal advantage of SR is the small size of the electron beam, thereby providing a high-intensity x-ray point source. Using a nearly parallel beam of SR, along with a precise detection system (pixel size of 4.5 μm), allowed us to obtain high-quality angiographic images with excellent spatial resolution. Furthermore, setting SR at an energy level just above the K absorption of barium produced the highest contrast images. SR imaging provides a powerful tool to reveal the morphology of small cerebral arteries such as superficial and deep penetrating arteries, allowing analysis of their physiologic and pathologic properties under a variety of conditions (ie, borderzone in infarction[23,24] and microaneurysm formation).

Fluorescence microscopy is another tool potentially useful for analysis of the microcirculation.[25] Although fluorescence microscopy provides visualization of microcirculation at the brain surface, the advantage of SR imaging is visualization of small vessels that have penetrated into the brain parenchyma, such as the subcortex. In addition, SR imaging allows performance of microangiography with an optimal projection. When the latter is combined with a microinjector, sequential real-time images can be obtained, providing the substrate for hemodynamic analysis.

In this article, we investigated SR imaging after stroke and showed that the SR image reflects pathologic changes previously observed by using anatomic/microscopic analysis. On day 9 after MCA occlusion, arteries on the surface of the cerebrum were visualized by SR, though penetrating intracerebral arteries were not detected. Previous studies have shown that the integrity of the distal cortical artery is usually maintained after occlusion of the proximal artery and that collateral flow is established through expansion of previously existing and/or formation of new vascular channels.[25,26] Analysis with enhanced MR imaging has shown cerebral parenchymal enhancement in the stroke area by 1 week after cerebral infarction,[27] indicative of blood flow in the peri-ischemic area. In contrast, penetrating intracerebral arteries were dramatically decreased in number in the ischemic hemisphere, though cortical branches on the brain surface were maintained after MCA occlusion. It has previously been shown that microvasculature in the ischemic territory displays adhesion of polymorphonuclear leukocytes in postcapillary venules, followed by the disruption of the microvascular network.[28] These previous findings are consistent with the results of our vascular images obtained by SR after ligation of the MCA.

Conclusion

Our study demonstrates, for the first time, the morphologic features of small vascular networks in murine brain by microangiography by using SR imaging. Our approach provides a powerful tool for evaluating potential angiogenic/antiangiogenic therapeutic strategies, as well as pathologic examination of the cerebral microarterial tree.

Acknowledgments

We thank Y. Kasahara, K. Tomiyasu, and M. Aoki for technical assistance.

References

1. Phillips SJ, Whisnant JP. **Hypertension and the brain: The National High Blood Pressure Education Program.** *Arch Intern Med* 1992;152:938–45
2. Ito K, Tanaka E, Mori H, et al. **A microangiographic technique using synchrotron radiation to visualize dermal circulation in vivo.** *Plast Reconstr Surg* 1998;102:1128–33
3. Tokiya R, Umetani K, Imai S, et al. **Observation of microvasculatures in athymic nude rat transplanted tumor using synchrotron radiation microangiography system.** *Academic Radiology* 2004;9:1039–46
4. Takeshita S, Isshiki T, Mori H, et al. **Use of synchrotron radiation microangiography to assess development of small collateral arteries in a rat model of hindlimb ischemia.** *Circulation* 1997;95:805–08
5. Conway JG, Popp JA, Thurman RG. **Microcirculation in periportal and pericentral regions of lobule in perfused rat liver.** *Am J Physiol* 1985;249:G449–56
6. Stock RJ, Cilento EV, McCuskey RS. **A quantitative study of fluorescein isothiocyanate-dextran transport in the microcirculation of the isolated perfused rat liver.** *Hepatology* 1989;9:75–82
7. Birngruber R, Schmidt-Erfurth U, Teschner S, et al. **Confocal laser scanning fluorescence topography: a new method for three-dimensional functional imaging of vascular structures.** *Graefes Arch Clin Exp Ophthalmol* 2000;238:559–65
8. Mori H, Hyodo K, Tanaka E, et al. **Small-vessel radiography in situ with monochromatic synchrotron radiation.** *Radiology* 1996;201:173–77
9. Umetani K, Yagi N, Suzuki Y, et al. **Observation and analysis of microcirculation using high-spatial-resolution image detectors and synchrotron radiation.** *Proceeding of SPIE* 2000;3977:522–33
10. Yamashita T, Kawashima S, Ozaki M, et al. **Images in cardiovascular medicine: mouse coronary angiograph using synchrotron radiation microangiography.** *Circulation* 2002;105:E3–4
11. Kuzmiak CM, Pisano ED, Cole EB, et al. **Comparison of full-field digital mammography to screen-film mammography with respect to contrast and spatial resolution in tissue equivalent breast phantoms.** *Med Phys* 2005;32:3144–50
12. Taguchi A, Soma T, Tanaka H, et al. **Administration of CD34+ cells after stroke enhances neurogenesis via angiogenesis in a mouse model.** *J Clin Invest* 2004;114:330–38
13. Furuya K, Kawahara N, Kawai K, et al. **Proximal occlusion of the middle cerebral artery in C57Black6 mice: relationship of patency of the posterior communicating artery, infarct evolution, and animal survival.** *J Neurosurg* 2004;100:97–105
14. Kitagawa K, Matsumoto M, Mabuchi T, et al. **Deficiency of intercellular adhesion molecule 1 attenuates microcirculatory disturbance and infarction size in focal cerebral ischemia.** *J Cereb Blood Flow Metab* 1998;18:1336–45
15. Matsushita K, Matsuyama T, Nishimura H, et al. **Marked, sustained expression of a novel 150-kDa oxygen-regulated stress protein, in severely ischemic mouse neurons.** *Brain Res Mol Brain Res* 1998;60:98–106
16. Coyne EF, Ngai AC, Meno JR, et al. **Methods for isolation and characterization of intracerebral arterioles in the C57/BL6 wild-type mouse.** *J Neurosci Methods* 2002;120:145–53
17. Herman LH, Ostrowski AZ, Gurdjian ES. **Perforating branches of the middle cerebral artery: an anatomical study.** *Arch Neurol* 1963;8:32–34
18. Kaplan HA. **The lateral perforating branches of the anterior and middle cerebral arteries.** *J Neurosurg* 1965;23:305–10
19. de Reuck J. **The area of the deep perforating branches of the median cerebral artery in man** [in French]. *Acta Anat (Basel)* 1969;74:30–35
20. Salamon G, Combalbert A, Faure J, et al. **Microradiographic study of the arterial circulation of the brain.** *Prog Brain Res* 1968;30:33–41
21. Mori H, Hyodo K, Tobita K, et al. **Visualization of penetrating transmural arteries in situ by monochromatic synchrotron radiation.** *Circulation* 1994;89:863–71
22. Salamon G, Raybaud C, Michotey P, et al. **Angiographic study of cerebral convolutions and their area of vascularization** [in French]. *Rev Neurol (Paris)* 1975;131:259–84
23. Bogousslavsky J, Regli F. **Centrum ovale infarcts: subcortical infarction in the superficial territory of the middle cerebral artery.** *Neurology* 1992;42:1992–98
24. Donnan GA, Norrving B, Bamford JM, et al. **Subcortical infarctions: classification and terminology.** *Cerebrovasc Dis* 1993;3:248–51
25. Tomita Y, Kubis N, Calando Y, et al. **Long-term in vivo investigation of mouse cerebral microcirculation by fluorescence confocal microscopy in the area of focal ischemia.** *J Cereb Blood Flow Metab* 2005;25:858–67
26. Zulch KJ. *Cerebral Circulation and Stroke.* Berlin, Germany: Springer-Verlag; 1971:116
27. Merten CL, Knitelius HO, Assheuer J, et al. **MRI of acute cerebral infarcts: increased contrast enhancement with continuous infusion of gadolinium.** *Neuroradiology* 1999;41:242–48
28. del Zoppo GJ, Mabuchi T. **Cerebral microvessel responses to focal ischemia.** *J Cereb Blood Flow Metab* 2003;23:879–94

Journal of Cerebral Blood Flow & Metabolism (2008) 28, 445–449

www.jcbfm.com

Brief Communication

Circulating CD34-positive cells provide a marker of vascular risk associated with cognitive impairment

Akihiko Taguchi[1], Tomohiro Matsuyama[2], Takayuki Nakagomi[2], Yoko Shimizu[1], Ryuzo Fukunaga[3], Yoshiaki Tatsumi[4], Hiroo Yoshikawa[4], Akie Kikuchi-Taura[5], Toshihiro Soma[5], Hiroshi Moriwaki[1], Kazuyuki Nagatsuka[1], David M Stern[6] and Hiroaki Naritomi[1]

[1]*Department of Cerebrovascular Disease, National Cardiovascular Center, Osaka, Japan;* [2]*Institute for Advanced Medical Sciences, Hyogo College of Medicine, Hyogo, Japan;* [3]*Department of Cerebrovascular Disease, Hoshigaoka Koseinenkin Hospital, Osaka, Japan;* [4]*Department of Internal Medicine, Hyogo College of Medicine, Hyogo, Japan;* [5]*Department of Hematology, Osaka Minami National Medical Center, Osaka, Japan;* [6]*Dean's Office, College of Medicine, Cincinnati University, Cincinnati, Ohio, USA*

Maintenance of uninterrupted cerebral circulation is critical for neural homeostasis. The level of circulating CD34-positive (CD34$^+$) cells has been suggested as an index of cerebrovascular health, although its relationship with cognitive function has not yet been defined. In a group of individuals with cognitive impairment, the level of circulating CD34$^+$ cells was quantified and correlated with clinical diagnoses. Compared with normal subjects, a significant decrease in circulating CD34$^+$ cells was observed in patients with vascular-type cognitive impairment, although no significant change was observed in patients with Alzheimer's-type cognitive impairment who had no evidence of cerebral ischemia. The level of cognitive impairment was inversely correlated with numbers of circulating CD34$^+$ cells in patients with vascular-type cognitive impairment, but not Alzheimer's type. We propose that the level of circulating CD34$^+$ cells provides a marker of vascular risk associated with cognitive impairment, and that differences in the pathobiology of Alzheimer's- and vascular-type cognitive impairment may be mirrored in levels of circulating CD34$^+$ cells in these patient populations.
Journal of Cerebral Blood Flow & Metabolism (2008) **28,** 445–449; doi:10.1038/sj.jcbfm.9600541; published online 8 August 2007

Keywords: antigens; CD34; cerebral circulation; cognitive impairment

Introduction

Maintaining integrity of the cerebral circulation has a critical role in neural homeostasis. Although analysis of risk factors for cerebrovascular disease has certainly provided insights into mechanisms of vascular disease, it is still difficult to predict accurately the contribution of vascular dysfunction in the long-term outcome of acute vascular insufficiency or in chronic neurodegenerative disorders. For example, in Alzheimer's disease (Casserly and Topol, 2004; Vagnucci and Li, 2003), assessment of a possible vascular component in the pathogenesis of neuronal degeneration is often ambiguous during a patient's lifetime.

Repair of the cerebral microcirculation has traditionally been assigned to ongoing replacement of damaged cerebral endothelium from outgrowth of preexisting vasculature. However, recent studies have identified circulating bone marrow-derived immature cells, including CD34-positive (CD34$^+$) cells, as contributors in maintenance of the vasculature; they have the potential to serve as a pool of endothelial progenitor cells (Asahara *et al*, 1997) and as a source of growth/angiogenesis factors (Majka *et al*, 2001). In a previous study, we have shown that circulating CD34$^+$ cells provide an index of cerebrovascular function (Taguchi *et al*, 2004*a*). We have also found that in a model of experimental cerebral ischemia, intravenous administration of CD34$^+$ cells improved neurologic function, at least in part, by restoring cerebral microcirculation in the ischemic area (Taguchi *et al*, 2004*b*).

Correspondence: Dr A Taguchi, Department of Cerebrovascular Disease, National Cardiovascular Center, 5-7-1 Fujishiro-dai, Suita, Osaka 565-8565, Japan.
E-mail: taguchi@ri.ncvc.go.jp
This work was supported by Grant-in-Aid for Scientific Research from the Ministry of Health, Labour, and Welfare.
Received 7 June 2007; revised 1 July 2007; accepted 2 July 2007; published online 8 August 2007

These results lead us to propose that circulating immature vascular progenitor cells contribute to neural homeostasis, at least in part, through their role in maintaining cerebral microvascular function. Using a recently developed method that allows precise measurement of the CD34+ cell population in peripheral blood (Kikuchi-Taura *et al*, 2006), we have evaluated the level of circulating CD34+ cells in patients with impaired neurologic function of diverse etiologies. Our goal has been to determine if there is relationship between levels of CD34+ cells, impaired neural function, and vascular integrity.

Materials and methods

This study was approved by Institutional Review Boards of the respective institutions (National Cardiovascular Center, Hyogo College of Medicine, Hoshigaoka Koseinenkin Hospital, and Osaka Minami National Medical Center). All subjects provided informed consent. Individuals with Mini Mental State Examination Score (MMSE) <24 and Clinical Dementia Rating (CDR) ≥ 0.5 were enrolled in this study and defined as having impaired cognitive function. In the view of history, evaluation of symptoms, and results of brain imaging studies (magnetic resonance imaging and single photon-computed tomography), patients with cognitive impairment were divided into two groups by neurologists blinded to the experimental protocol: vascular-type cognitive impairment or Alzheimer's-type cognitive impairment, according to the criteria of *Diagnostic and Statistical Manual of Mental Disorders* (4th ed, DSM-4) (American Psychiatric Association, 1994). To exclude the contribution of vascular element in patients with Alzheimer's-type cognitive impairment, patients' coexistent Alzheimer's-type cognitive impairment and cerebral infarction, observed by magnetic resonance imaging, were excluded from this study. In addition, patients with cognitive impairment diagnosed as neither of the Alzheimer's type nor vascular type were excluded. A total of 95 individuals, including 32 age-matched control subjects with no history of vascular disease, no neuronal deficiency, and no cognitive impairment, were enrolled. In addition, individuals excluded from the study included: premenopausal women, patients who experienced a vascular event within 30 days of measurements, history of cerebral hemorrhage, and evidence of infection or malignant disease. Using a modification of the International Society of Hematotherapy and Graft Engineering (ISHAGE) Guidelines (Sutherland *et al*, 1996), the number of circulating CD34+ cells was quantified as described (Kikuchi-Taura *et al*, 2006). In brief, blood samples were incubated with phycoerythrin-labeled anti-CD34 antibody, fluorescein isothiocyanate-labeled anti-CD45 antibody, 7-aminoactinomycin-D, and internal control (all of these reagents are from the Stem-Kit, Beckman Coulter, Marseille, France). 7-Aminoactinomycin-D-positive dead cells and CD45-negative cells were excluded, and the number of cells forming a cluster with characteristic CD34+ cells (i.e., low side scatter and low-to-intermediate CD45 staining) was counted. The absolute number of CD34+ cells was calculated using the internal control. In this study, we used a single measurement at the time of entry into the study, on the basis of our previous observation that the level of circulating CD34+ cells is relatively stable (Taguchi *et al*, 2004*a*). For statistical analysis, JMP version 5.1J (SAS Institute Inc, Co, NC, USA) was used. Individual comparisons were performed using a two-tailed, unpaired Students' *t*-test. Statistical comparisons among groups were determined using analysis of variance. Mean $\pm$ s.e. is shown.

Results

Baseline characteristics of the groups are shown in Table 1. In univariate analysis of control subjects, each cerebrovascular risk factor and other treatment showed no significant difference with the number of circulating CD34+ cells (data not shown).

To investigate a possible relationship between circulating CD34+ cells and cognition, the level of circulating CD34+ cells was compared among these groups. Representative fluorescence-activated cell sorting images are shown in Figure 1A (vascular-type) and 1B (Alzheimer's-type). Analysis of variance revealed a significant decrease of CD34+ cells in patients with vascular-type cognitive impairment compared with Alzheimer's-type cognitive impairment ($P<0.001$) and normal subjects ($P<0.001$, Figure 1C).

To investigate further a possible association of circulating CD34+ cells with cognitive impairment, patients with vascular-type impaired cognition were divided into two groups according to their CDR (mild: CDR = 0.5, $n=22$, mean age = 75.2 $\pm$ 1.6 years; moderate-severe: CDR $\geq$ 1, $n=18$, mean age = 75.3 $\pm$ 1.5 years) or MMSE (mild: MMSE $\geq$ 20, $n=25$, mean age = 74.2 $\pm$ 1.4 years; moderate-severe: MMSE $<$ 20, $n=15$, mean age = 77.1 $\pm$ 1.5 years). The results showed a significant decrease in the level of circulating CD34+ cells in moderate-severe group, based on stratification by either CDR (Figure 1D, $P=0.01$) or MMSE (Figure 1E, $P=0.03$) in patients with vascular-type cognitive impairment. Similar analysis was applied to patients with Alzheimer's-type impaired cognition. They were divided into two groups according to CDR (mild: $n=8$, mean age = 73.0 $\pm$ 4.7 years; moderate-severe: $n=15$, mean age = 77.5 $\pm$ 1.9 years) or MMSE (mild: $n=12$, mean age = 74.1 $\pm$ 3.0 years; moderate-severe: $n=11$, mean age = 77.8 $\pm$ 2.9 years). However, in contrast to patients with vascular-type impaired cognition, there was no significant difference observed in patients with Alzheimer's-type cognitive impaired, based on CDR (Figure 1F, $P=0.86$) or MMSE (Figure 1G, $P=0.60$).

Discussion

Our results are consistent with a contribution of circulating CD34+ cells in support of cognitive function, presumably through their positive homeostatic influence on the cerebral circulation in

Table 1 Baseline characteristics

		Cognitive impairment			
	Total	*Vascular-type*	*Alzheimer's-type*	*Control*	*P-value for trend*
n	95	40	23	32	
Age, years	74.9±0.6	75.3±1.1	75.9±2.1	74.2±0.7	0.53
Male gender, *n* (%)	57 (60)	27 (68)	12 (52)	18 (56)	0.46
Risk factor, n (%)					
Hypertension	41 (43)	21 (53)	9 (39)	11 (34)	0.28
Hyperlipidemia	29 (31)	14 (35)	5 (22)	10 (31)	0.53
Diabetes mellitus	9 (9)	5 (13)	1 (4)	3 (9)	0.57
Smoking	20 (21)	10 (25)	6(26)	4 (13)	0.34
Treatment, n (%)					
Ca-channel blocker	30 (32)	15 (38)	6 (26)	9 (28)	0.56
β-Blocker	2 (2)	1 (3)	0 (0)	1 (3)	0.71
ACE inhibitor	4 (4)	3 (8)	1 (4)	0 (0)	0.29
ARB	8 (8)	3 (8)	3 (13)	2 (6)	0.65
Diuretics	6 (6)	2 (5)	1 (4)	3(9)	0.68
Statin	29 (31)	14 (35)	5 (22)	10 (31)	0.54
Aspirin	28 (29)	23 (58)	1 (4)	4 (13)	<0.01
Ticlopidine	11(12)	9 (23)	0 (0)	2 (6)	0.01

ACE, angiotensin-converting enzyme; ARB, angiotensin II receptor blocker.

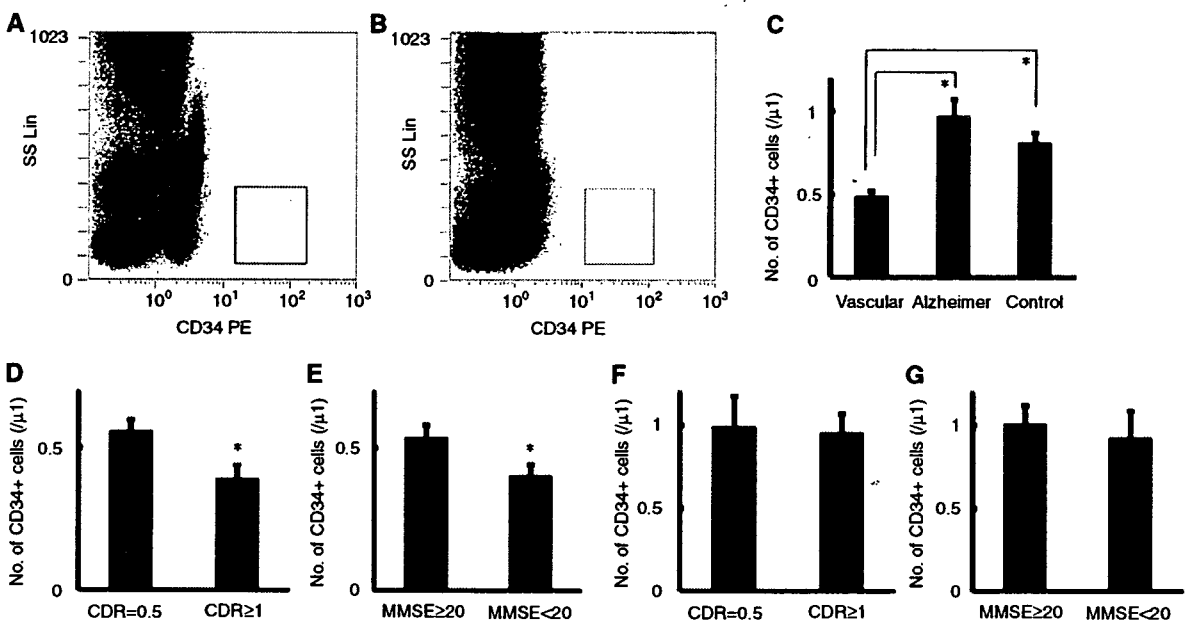

Figure 1 Levels of circulating CD34+ cells and cognitive impairment. (**A** and **B**) After exclusion of 7-AAD-positive dead cells and CD45-negative cells (non-leukocyte), CD34+ cells cluster at low side scatter were clearly observed (**A**, vascular-type; **B**, Alzheimer's-type). (**C**) Analysis of variance revealed a significant decrease in circulating CD34+ cells in patients with vascular-type cognitive impairment compared with normal subjects and individuals with Alzheimer's-type cognitive impairment. In contrast, no significant change in circulating CD34+ cells was observed in patients with Alzheimer's-type cognitive impairment compared with control subjects. (**D** and **E**) In the group of patients with vascular-type cognitive impairment, the level of circulating CD34+ cells was significantly reduced in patients with more severe cognitive impairment compared with the more mildly affected group (**D**, CDR; **E**, MMSE). (**F** and **G**) In contrast, no significant difference was observed in patients with Alzheimer's-type cognitive impairment based on assessment of cognition (**F**, CDR; **G**, MMSE). SS Lin, side-scatter linear scale. $*P < 0.05$.

settings of ischemic stress. Further, these observations suggest a basic difference between the pathobiology of dementia in Alzheimer's disease (without associated cerebral ischemia) and declining cognitive function in patients with ischemic cerebrovascular disorders.

Late onset, sporadic Alzheimer's disease is a heterogeneous disorder (Casserly and Topol, 2004) and the contribution of a vascular factor is still controversial. In contrast to vascular-type cognitive impairment, no significant change (at most, a mild increase) in the level of circulating $CD34^+$ cells was observed in patients with Alzheimer's-type cognitive impairment who had no cerebral ischemia. Consistent with a $CD34^+$ cell-independent mechanism of cognitive decline in Alzheimer's-type impaired cognition, there was no correlation between circulating $CD34^+$ cells and the level of CDR or MMSE. These results suggest that the level of $CD34^+$ cells in the peripheral circulation might provide a useful means of separating dementia with a vascular etiology from dementia associated with nonvascular causes. This is not inconsistent with a previous report indicating decreased levels of $CD34^+$ cells in patients with early Alzheimer's disease that did not exclude patients with coexisting cerebral ischemia (Maler *et al*, 2006). Our findings could have implications for treatment, especially as more modalities become available for patients with declining cognitive function.

The level of circulating endothelial progenitor cells, identified based on positivity for CD34 and kinase insert domain receptor ($CD34^+/KDR^+$ cells), has been correlated with cardiovascular risk factors (Vasa *et al*, 2001) and cardiovascular outcomes (Schmidt-Lucke *et al*, 2005; Werner *et al*, 2005). However, large variations in the levels of $CD34^+/KDR^+$ cells in the latter reports (by ~100-fold between reports; Fadini *et al*, 2006; Werner *et al*, 2005) indicate the need to standardize this measurement. In contrast, in our study, although there was no strong correlation between levels of $CD34^+$ cells and established cardiovascular risk factors and other treatments, probably because of the heterogeneity of our control subjects, the results indicate a close relationship between the overall $CD34^+$ pool and the cognitive impairment with cerebral ischemia. Previous reports have indicated a positive correlation between mobilization of $CD34^+$ cells and improved functional outcome in stroke patients (Dunac *et al*, 2007). Accelerated functional recovery after experimental stroke, because of administration of $CD34^+$ cells (Shyu *et al*, 2006; Taguchi *et al*, 2004*b*), suggests the possible contribution of $CD34^+$ cells in maintenance of brain function during cerebral circulation. Our method for quantification of $CD34^+$ cells is simple, reproducible (Kikuchi-Taura *et al*, 2006), and suitable for screening a broad group of patients at risk for cerebrovascular disorders.

In conclusion, our results indicate that the level of circulating $CD34^+$ cells provides a marker of vascular risk associated with cognitive impairment. Furthermore, differences in the pathobiology of Alzheimer's- and vascular-type cognitive impairment may be mirrored in levels of circulating $CD34^+$ cells in these patient populations.

Acknowledgements

We thank Y Kasahara, K Obata, and Y Okinaka for technical assistance.

Conflict of interest

The authors state no conflict of interest.

References

American Psychiatric Association (1994) *Diagnostic and statistical manual of mental disorders*. 4th ed Washington, DC: American Psychiatric Association

Asahara T, Murohara T, Sullivan A, Silver M, van der Zee R, Li T, Witzenbichler B, Schatteman G, Isner JM (1997) Isolation of putative progenitor endothelial cells for angiogenesis. *Science* 275:964–7

Casserly I, Topol E (2004) Convergence of atherosclerosis and Alzheimer's disease: inflammation, cholesterol, and misfolded proteins. *Lancet* 363:1139–46

Dunac A, Frelin C, Popolo-Blondeau M, Chatel M, Mahagne MH, Philip PJ (2007) Neurological and functional recovery in human stroke are associated with peripheral blood CD34+ cell mobilization. *J Neurol* 254:327–32

Fadini GP, Coracina A, Baesso I, Agostini C, Tiengo A, Avogaro A, de Kreutzenberg SV (2006) Peripheral blood CD34+KDR+ endothelial progenitor cells are determinants of subclinical atherosclerosis in a middle-aged general population. *Stroke* 37:2277–82

Kikuchi-Taura A, Soma T, Matsuyama T, Stern DM, Taguchi A (2006) A new protocol for quantifying CD34+ cells in peripheral blood of patients with cardiovascular disease. *Texas Heart Inst J* 33:427–9

Majka M, Janowska-Wieczorek A, Ratajczak J, Ehrenman K, Pietrzkowski Z, Kowalska MA, Gewirtz AM, Emerson SG, Ratajczak MZ (2001) Numerous growth factors, cytokines, and chemokines are secreted by human CD34(+) cells, myeloblasts, erythroblasts, and megakaryoblasts and regulate normal hematopoiesis in an autocrine/paracrine manner. *Blood* 97: 3075–85

Maler JM, Spitzer P, Lewczuk P, Kornhuber J, Herrmann M, Wiltfang J (2006) Decreased circulating CD34+ stem cells in early Alzheimer's disease: evidence for a deficient hematopoietic brain support? *Mol Psychiatry* 11:1113–5

Schmidt-Lucke C, Rossig L, Fichtlscherer S, Vasa M, Britten M, Kamper U, Dimmeler S, Zeiher AM (2005) Reduced number of circulating endothelial progenitor cells predicts future cardiovascular events: proof of concept for the clinical importance of endogenous vascular repair. *Circulation* 111:2981–7

Shyu WC, Lin SZ, Chiang MF, Su CY, Li H (2006) Intracerebral peripheral blood stem cell (CD34+) implantation induces neuroplasticity by enhancing beta1 integrin-mediated angiogenesis in chronic stroke rats. *J Neurosci* 26:3444–53

Sutherland DR, Anderson L, Keeney M, Nayar R, Chin-Yee I (1996) The ISHAGE guidelines for CD34+ cell determination by flow cytometry. International Society of Hematotherapy and Graft Engineering. *J Hematother* 5:213–26

Taguchi A, Matsuyama T, Moriwaki H, Hayashi T, Hayashida K, Nagatsuka K, Todo K, Mori K, Stern DM, Soma T, Naritomi H (2004*a*) Circulating CD34-positive cells provide an index of cerebrovascular function. *Circulation* 109:2972–5

Taguchi A, Soma T, Tanaka H, Kanda T, Nishimura H, Yoshikawa H, Tsukamoto Y, Iso H, Fujimori Y, Stern DM, Naritomi H, Matsuyama T (2004*b*) Administration of CD34+ cells after stroke enhances neurogenesis via angiogenesis in a mouse model. *J Clin Invest* 114: 330–8

Vagnucci Jr AH, Li WW (2003) Alzheimer's disease and angiogenesis. *Lancet* 361:605–8

Vasa M, Fichtlscherer S, Aicher A, Adler K, Urbich C, Martin H, Zeiher AM, Dimmeler S (2001) Number and migratory activity of circulating endothelial progenitor cells inversely correlate with risk factors for coronary artery disease. *Circ Res* 89:E1–7

Werner N, Kosiol S, Schiegl T, Ahlers P, Walenta K, Link A, Bohm M, Nickenig G (2005) Circulating endothelial progenitor cells and cardiovascular outcomes. *New Engl J Med* 353:999–1007